Journal of Applied Analysis and Computation
Volume 9, Number 3, June 2019, 1132–1164
Website:http://jaac.ijournal.cn
DOI:10.11948/2156-907X.20190015

TURING-HOPF BIFURCATION IN THE REACTION-DIFFUSION SYSTEM WITH DELAY AND APPLICATION TO A DIFFUSIVE PREDATOR-PREY MODEL*

Yongli Song[1,†], Heping Jiang[2] and Yuan Yuan[3]

Abstract The interactions of diffusion-driven Turing instability and delay-induced Hopf bifurcation always give rise to rich spatiotemporal dynamics. In this paper, we first derive the algorithm for the normal forms associated with the Turing-Hopf bifurcation in the reaction-diffusion system with delay, which can be used to investigate the spatiotemporal dynamical classification near the Turing-Hopf bifurcation point in the parameter plane. Then, we consider a diffusive predator-prey model with weak Allee effect and delay. Through investigating the dynamics of the corresponding normal form of Turing-Hopf bifurcation induced by diffusion and delay, the spatiotemporal dynamics near this bifurcation point can be divided into six categories. Especially, stable spatially homogeneous/inhomogeneous periodic solutions and steady states, coexistence of two stable spatially inhomogeneous periodic solutions, coexistence of two stable spaially inhomogeneous steady states and the transition from one kind of spatiotemporal patterns to another are found.

Keywords Diffusion, delay, Turing-Hopf bifurcation, normal form, predator-prey model.

MSC(2010) 35B10, 35B32, 35B35, 35K57, 35R10.

1. Introduction

Since Alan Turing proposed a reaction-diffusion (RD) system to explain how diffusion motivates the spatial patterns in the morphological phenomena [38], diffusion-driven instability (known as Turing instability) has been widely studied and the reaction-diffusion model acts gradually as a framework for understanding biological pattern formation [21, 39]. Numerical analysis and simulations have shown that a surprising variety of irregular spatiotemporal patterns can occcur even for a simple reaction-diffusion model [26].

[†]the corresponding author. Email address:songyl@hznu.edu.cn (Y. Song)
[1]Department of Mathematics, Hangzhou Normal University, Hangzhou 311121, China
[2]School of Mathematics and Statistics, Huangshan University, Anhui, 245041, China
[3]Department of Mathematics and Statistics, Memorial University of Newfoundland, St. John's, Newfoundland, A1C 5S7, Canada
[*]The authors were supported by National Natural Science Foundation of China (11571257,11701208), the Science and Technology Commission of Shanghai Municipality (STCSM) (18dz2271000) and Zhejiang Provincial Natural Science Foundation of China (LY19A010010).

On the unbounded domain, the travelling wave solutions of the RD system have been widely investigated [40,46]. On the bounded domain, the effect of the boundary condition on the dynamcis of the RD system is discussed in the framework of bifurcation theory [14,23]. There are many works dealling with the Hopf bifurcaion and Turing bifurcation in a wide variety of fields like the biological and ecological systems [22,27–29,31,37,41,49], biochemical system [6,7,18]. Interactions between different bifiurcations can result in particularly complex patterns. The complex spatiotemporal patterns due to interaction between Turing and Hopf bifurcations (known as Turing-Hopf bifurcation) have been studied in [19,20,32,48]. In [34], the authors derived the algorithm of calculating the norm form associated with the Turing-Hopf bifurcation for a general RD system and found that stable spatially inhomogeneous periodic solutions emerge because of the interaction between Turing and Hopf bifurcations, which are periodic in both space and time. These stable spatially inhomogeneous periodic solutions are different from the classic Turing patterns [38], which are periodic in space but stationary in time. Interaction between Turing bifurcations (known as spatial resonances or Turing-Turing bifurcation or Bogdanov-Takens bifurcation) have been discussed in [19,45,47]. For more works on bifurcation theory of RD system, see the excellent monographs by Haragus and Iooss [14] and Mei [23].

In addition, there are many reasons of introducing time delay into the real biological or biochemical systems such as the maturation delay and digestion delay in the population system, time delay due to the process of transcription and translation in physiology and the delay during the chemical reaction. The system with delay means that the evolution of system depends on not only the present but also the historical information. In terms of various modeling mechanisms, discrete delay, distributed delay, nonlocal delay and spatiotemporal delay are often involved in the literatures. For the Neumann boundary condition, the influence of delay on the stability of the positive homogeneous steady state and delay-induced Hopf bifurcation have been investigated in [9,16,24,36,50]. The main result of these studies show that delay can induce the stable spatially homogeneous periodic solution and the first critical value is the same to that in the corresponding local system (the system without diffusion). For the Direchlet boundary condition, the stability of the positive spatially inhomogeneous steady state and delay-induced Hopf bifurcation are investigated in [1,3,11,12,15,30,35]. The stability and direction of Hopf bifurcation can be determined by calculating the corresponding normal forms. In [8], Faria developed the normal form theory for partial functional differential equations near equilibrium points and studied the qualitative behavior of solutions when a Hopf bifurcation occurs. The Bogdanov-Takens bifurcations in the reaction-diffusion with delay have been studied in [2,42].

However, there are few works on Turing-Hopf bifurcation in the RD system with delay. Hadeler and Ruan [13] have studied the joint effects of diffusion and delay and pointed out that it would be very interesting to study the Turing-Hopf bifurcation in the delayed diffusive predator-prey model. In [33], Song and Jiang derived the algorithm of the normal form for the zero-Hopf bifurcation for a general system with delay but without diffusion. Motivated by the works in [8,13,33,34], in this paper, we investigate the dynamics aroused by the interaction between the diffusion-driven Turing instability and delay-induced Hopf bifurcation. The reseach is based on the calculation of normal form for Turing-Hopf bifurcation. Although the normal form theory for partial functional differential equations has been developed in [8], the explicit expression of the coefficient of the normal form of the Turing-Hopf bifurcation depending on the original system has not been derived. We first derive the algorithm of calculating the normal form of Turing-Hopf bifurcation for the general raction-diffusion system with delay and obtain the explicit expression of the coefficients up to third-order terms of the normal form, which can be determined by the coefficients of second and third terms of the original system. Then, applying the obtained general theoretical results to a diffusive predator-prey model with weak Allee effect and delay, the coefficiens of the normal form can be explicitly given in terms of the coefficients of the original system and obtain dynamical classification near the Turing-Hopf bifurcation point. We would like to mention that partial of the work presented in this paper is based on Heping Jiang's doctoral dissertation in 2016, while similar project has also been studied in [17]. The theoretical results obtained in both of this manuscript and [17] are general extension of [34] from the RD system without delay to delay case.

This paper is organized as follows. In Section 2, we derive the algorithm of calculating the normal form of Turing-Hopf bifurcation for the general raction-diffusion system with delay. In Section 3, we investigate the dynamics of diffusive predator-prey model with weak Allee effect and delay. We end the paper with a conclusion.

2. Normal forms of Turing-Hopf bifurcation in the reaction-diffusion system with delay

We consider the following reaction-diffusion system with delay

$$\frac{\partial u(x,t)}{\partial t} = d\Delta u(x,t) + G(u(x,t), u(x,t-\tau), \delta), \quad x \in (0, \ell\pi), t > 0, \tag{2.1}$$

where $u(x,t) = (u_1(x,t), u_2(x,t), \cdots, u_n(x,t))^T$,

$$d\Delta = \text{diag}\ \left\{d_1 \frac{\partial^2}{\partial x^2}, d_2 \frac{\partial^2}{\partial x^2}, \cdots, d_n \frac{\partial^2}{\partial x^2}\right\},\ G = (G_1, G_2, \cdots, G_n)^T,$$

$G(0,0,\delta) = 0$, $\tau > 0$ and $\delta > 0$ are parameters.

In the following, we investigate the Turing-Hopf bifurcation for system (2.1) with the Neumann boundary condition $\frac{\partial u(x,t)}{\partial x}\Big|_{x=0,\ell\pi} = 0, t > 0$. Obviously, $u = 0$ is always a solution. The characteristic equation of the linearized system of system (2.1) at $u = 0$ is

$$\prod_{k\in\mathbb{N}_0} \Gamma_k(\lambda) = 0, \tag{2.2}$$

where $\mathbb{N}_0 = \{0, 1, 2, \cdots\}$, $\Gamma_k(\lambda) = \det(\mathcal{M}_k(\lambda))$ with

$$\mathcal{M}_k(\lambda) = \lambda I_n + \text{diag}\left\{d_1\left(\frac{k}{\ell}\right)^2, d_2\left(\frac{k}{\ell}\right)^2, \cdots, d_n\left(\frac{k}{\ell}\right)^2\right\} - A_{0,\delta} - A_{1,\delta}e^{-\lambda\tau}, \tag{2.3}$$

where I_n is an $n \times n$ identity matrix, $A_{0,\delta} = \frac{\partial G(0,0,\delta)}{\partial u(x,t)}$, $A_{1,\delta} = \frac{\partial G(0,0,\delta)}{\partial u(x,t-\tau)}$.

The notations used in this section are the same as in references [8,34]. For the codimension-2 Turing-Hopf singularity, we give the following assumption:

$(A1)$ when $(\delta,\tau)=(\delta_*,\tau_*)$, the equation $\Gamma_0(\lambda)=0$ has a pair of simple purely imaginary roots $\pm i\omega_*$, and there exists an integer $k=k_*\in\mathbb{N}=\{1,2,\cdots\}$ such that the equation $\Gamma_{k_*}(\lambda)=0$ has a simple zero root $\lambda=0$. In addition, the corresponding transversality condtion holds.

In what follows, set $\delta=\delta_*+\mu_1$ and $\tau=\tau_*+\mu_2$ such that μ_1 and μ_2 are perturbation parameters. Normalizing the delay by the time-scaling $t\to t/\tau$, defining the real-valued Sobolev space

$$\mathscr{X}=\left\{u\in\left(W^{2,2}(0,\ell\pi)\right)^n,\frac{\partial u_i}{\partial x}=0,x=0,\ell\pi,i=1,2,\cdots,n\right\},$$

and letting $\mathscr{C}:=C\left([-1,0];\mathscr{X}\right)$ be the Banach space of continuous mappings from $[-1,0]$ to $\mathscr{X}$ with the sup norm, system (2.1) becomes the following system on $\mathscr{C}$

$$\frac{\partial u(x,t)}{\partial t}=(\tau_*+\mu_2)d\Delta u(x,t)+L(\mu)(u_t(x,\theta))+F(u_t(x,\theta),\mu),\qquad(2.4)$$

where $u_t(x,\theta)\in\mathscr{X}$ for $u_t(x,\theta)=u(x,t+\theta),-1\le\theta\le 0$,

$$L(\mu)(u_t(x,\theta))=(\tau_*+\mu_2)\left(A_{0,\delta_*+\mu_1}u_t(x,0)+A_{1,\delta_*+\mu_1}u_t(x,-1)\right),\qquad(2.5)$$

$$F(u_t(x,\theta),\mu)=(\tau_*+\mu_2)G(u_t(x,0),u_t(x,-1),\delta_*+\mu_1)-L(\mu)(u_t(x,\theta)).\qquad(2.6)$$

Assume that V is a neighbourhood of zero in $\mathbb{R}^2$, and $F:\mathscr{C}\times V\to\mathscr{X}$ is a C^k function $(k\ge 2)$ with $F(0,\mu)=0,DF(0,\mu)=0$ for all $\mu=(\mu_1,\mu_2)\in V$, where $C^k=C^k\left([-1,0];\mathscr{X}\right)$ denotes the space of k times continuously differentiable functions from $[-1,0]$ to $\mathscr{X}$. Further, we write system (2.4) as the following form in which linear tems is separated from nonlinear terms

$$\frac{\partial u(x,t)}{\partial t}=\tau_*d\Delta u(x,t)+L_0(u_t(x,\theta))+\widetilde{F}(u_t(x,\theta),\mu),\qquad(2.7)$$

where

$$L_0(u_t(x,\theta))=L(0)(u_t(x,\theta))=\tau_*\left(A_{0,\delta_*}u_t(x,0)+A_{1,\delta_*}u_t(x,-1)\right)\qquad(2.8)$$

and

$$\widetilde{F}(u_t(x,\theta),\mu)=F(u_t(x,\theta),\mu)+L(\mu)\left(u_t(x,\theta)\right)-L_0\left(u_t(x,\theta)\right)+\mu_2 d\Delta u(x,t).\quad(2.9)$$

The linearized system of (2.7) is

$$\frac{\partial u(x,t)}{\partial t}=\tau_*d\Delta u(x,t)+L_0(u_t(x,\theta)).\qquad(2.10)$$

The characteristic equation of (2.10) is

$$\prod_{k\in\mathbb{N}_0}\widetilde{\Gamma}_k(\lambda)=0,\qquad(2.11)$$

where $\widetilde{\Gamma}_k(\lambda)=\det\left(\widetilde{\mathscr{M}}_k(\lambda)\right)$ with

$$\widetilde{\mathscr{M}}_k(\lambda)=\lambda I_n-\tau_*\mathrm{diag}\left\{\delta_k^{(1)},\delta_k^{(2)},\cdots,\delta_k^{(n)}\right\}-\tau_*A_{0,\delta_*}-\tau_*A_{1,\delta_*}e^{-\lambda},\qquad(2.12)$$

where $\delta_k^{(j)} = -d_j\left(\frac{k}{\ell}\right)^2, j = 1, 2, \cdots, n, k \in \mathbb{N}_0$.

It follows from the assumption $(A1)$ that the characteristic equation (2.11) has a pair of simple purely imaginary roots $\pm i\omega_c$ with $\omega_c = \omega_* \tau_*$ for $k = 0$, and has a simple zero root $\lambda = 0$ for $k = k_*$.

Let $C := C([-1, 0], \mathbb{R}^n), C^* := C([0, 1], \mathbb{R}^{n*})$, where $\mathbb{R}^{n*}$ is the $n-$dimensional space of row vectors, and define the adjoint bilinear form on $C^* \times C$ as follows

$$\langle\psi(s), \phi(\theta)\rangle = \psi(0)\phi(0) - \int_{-1}^{0}\int_{0}^{\theta} \psi(\xi - \theta)dM_k(\theta)\phi(\xi)d\xi, \ \ for \ \psi \in C^*, \phi \in C,$$

where $M_k \in BV([-1, 0]; \mathbb{R}^n)$ such that for $\phi(\theta) \in C$,

$$\mathrm{diag}\left\{\delta_k^{(1)}, \delta_k^{(2)}, \cdots, \delta_k^{(n)}\right\}\phi(0) + L_0(\phi(\theta)) = \int_{-1}^{0} dM_k(\theta)\phi(\theta).$$

Choosing

$$\Phi_1(\theta) = \left(\xi_0 e^{i\omega_c\theta}, \overline{\xi}_0 e^{-i\omega_c\theta}\right), \ \ \Phi_2(\theta) = \xi_{k_*},$$
$$\Psi_1(s) = \mathrm{col}\left(\eta_0^T e^{-i\omega_c s}, \overline{\eta}_0^T e^{i\omega_c s}\right), \ \ \Psi_2(s) = \eta_{k_*}^T,$$

where $\xi_0 \in \mathbb{C}^n$ and $\xi_{k_*} \in \mathbb{R}^n$ are the eigenvectors of system (2.10) associated with the eigenvalues $i\omega_c$ and 0, respectively, $\eta_0 \in \mathbb{C}^n$ and $\eta_{k_*} \in \mathbb{R}^n$ are the corresponding adjoint eigenvectors such that

$$\langle\Psi_1(s), \Phi_1(\theta)\rangle = I_2, \langle\Psi_2(s), \Phi_2(\theta)\rangle = 1.$$

For $u = (u_1, \cdots, u_n)^T, v = (v_1, \cdots, v_n)^T \in \mathscr{X}$, define the inner product $[\cdot, \cdot]$ as follows

$$[u, v] = \int_0^{l\pi} u^T v dx.$$

The eigenvalues of $\tau_* d\Delta$ on $\mathscr{X}$ are $\tau_*\delta_k^{(j)}$ with corresponding normalized eigenfunctions $\beta_k^{(j)}$ defined by

$$\beta_k^{(j)} = \gamma_k(x)e_j, \ \gamma_k(x) = \frac{\cos\left(\frac{kx}{\ell}\right)}{\|\cos\left(\frac{kx}{\ell}\right)\|_{2,2}} = \begin{cases} \frac{1}{\sqrt{\ell\pi}}, & \text{for } k = 0, \\ \frac{\sqrt{2}}{\sqrt{\ell\pi}}\cos\left(\frac{kx}{\ell}\right), & \text{for } k \neq 0, \end{cases}$$

where e_j is the unit coordinate vector of $\mathbb{R}^n$.

Following [8] and [34], define $\mathscr{C}_0^1 = \left\{\phi \in \mathscr{C} : \dot{\phi} \in \mathscr{C}, \phi(0) \in \mathrm{dom}(d\Delta)\right\}$ and let $\Phi(\theta) = \left(\Phi_1(\theta)\ \Phi_2(\theta)\right)$, $z_x = (z_1(t)\gamma_0(x), z_2(t)\gamma_0(x), z_3(t)\gamma_{k_*}(x))^T$. For $\varphi_t(x, \theta) \in \mathscr{C}_0^1$, we have the following decomposition

$$\varphi_t(x, \theta) = \Phi(\theta)z_x + w, \ \ w \in \mathscr{C}_0^1 \cap \mathrm{Ker}\pi := \mathscr{Q}^1. \tag{2.13}$$

Then, system (2.7) is decomposed as a system of abstract ODEs on $\mathbb{R}^3 \times \mathrm{Ker}\pi$

$$\begin{cases} \dot{z} = Bz + \Psi(0)\begin{pmatrix} \left[\widetilde{F}\left(\Phi(\theta)z_x + w, \mu\right), \beta_\nu^{(1)}\right] \\ \cdots \\ \left[\widetilde{F}\left(\Phi(\theta)z_x + w, \mu\right), \beta_\nu^{(n)}\right] \end{pmatrix}_{\nu=0}^{\nu=k_*}, \\ \dot{w} = A_{\mathscr{Q}^1}w + (I - \pi)X_0(\theta)\widetilde{F}\left(\Phi(\theta)z_x + w, \mu\right), \end{cases} \tag{2.14}$$

where $A_{\mathscr{Q}^1}: \mathscr{Q}^1 \to \mathrm{Ker}\pi$ is defined by

$$A_{\mathscr{Q}^1} w = \dot{w} + X_0(\theta)\left(L_0(w) + L_0^d(w) - \dot{w}(0)\right), \tag{2.15}$$

and $B = \mathrm{diag}\{i\omega_c, -i\omega_c, 0\}, \Psi(0) = \mathrm{diag}\{\Psi_1(0), \Psi_2(0)\}$.

In terms of the normal form theory of partial functional differential equations [8], after a recursive transformation of variables of the form

$$(z, w) = (\widetilde{z}, \widetilde{w}) + \frac{1}{j!}\left(U_j^1(\widetilde{z}, \mu), U_j^2(\widetilde{z}, \mu)\right), \quad j \geq 2,$$

where $z, \widetilde{z} \in \mathbb{R}^3, w, \widetilde{w} \in \mathscr{Q}^1$ and $U_j^1: \mathbb{R}^5 \to \mathbb{R}^3, U_j^2: \mathbb{R}^5 \to \mathscr{Q}^1$ are homogeneous polynomials of degree j in $\widetilde{z}$ and μ, the flow on the local center manifold for (2.14) is written as

$$\dot{z} = Bz + \sum_{j\geq 2} \frac{1}{j!} g_j^1(z, 0, \mu), \tag{2.16}$$

which is the normal form as in the usual sense for ODEs.

2.1. Calculation of $g_2^1(z, 0, \mu)$

The calculation of $g_2^1(z, 0, \mu)$ is very similar to that in [34]. Here, we simply give the results. Consider the formal Taylor expansion

$$L(\mu) = L_0 + \mu_1 L_1^{(1,0)} + \mu_2 L_1^{(0,1)} + \frac{1}{2}\left(\mu_1^2 L_2^{(2,0)} + 2\mu_1\mu_2 L_2^{(1,1)} + \mu_2^2 L_2^{(0,2)}\right) + \cdots, \tag{2.17}$$

$$F(v, \mu) = \frac{1}{2} F_2(v, \mu) + \frac{1}{3!} F_3(v, \mu) + \cdots, \tag{2.18}$$

where $F_j, j \geq 2$ is the jth Fréchet derivative of F. By (2.14), (2.17) and (2.18), we have

$$f_2^1(z, 0, \mu) = \Psi(0) \begin{pmatrix} \left[2\tilde{L}_1(\mu)\left(\Phi(\theta) z_x\right) + F_2\left(\Phi(\theta) z_x, \mu\right), \beta_\nu^{(1)}\right] \\ \cdots \\ \left[2\tilde{L}_1(\mu)\left(\Phi(\theta) z_x\right) + F_2\left(\Phi(\theta) z_x, \mu\right), \beta_\nu^{(n)}\right] \end{pmatrix}_{\nu=0}^{\nu=k_*}, \tag{2.19}$$

where

$$\tilde{L}_1(\mu) = L_1(\mu) + \mu_2 d\Delta = \mu_1 L_1^{(1,0)} + \mu_2 L_1^{(0,1)} + \mu_2 d\Delta.$$

For simplification of notations, we set

$$\mathcal{H}\left(\alpha z_1^{q_1} z_2^{q_2} z_3^{q_3} \mu_1^{\iota_1} \mu_2^{\iota_2}\right) = \begin{pmatrix} \alpha z_1^{q_1} z_2^{q_2} z_3^{q_3} \mu_1^{\iota_1} \mu_2^{\iota_2} \\ \overline{\alpha} z_1^{q_2} z_2^{q_1} z_3^{q_3} \mu_1^{\iota_1} \mu_2^{\iota_2} \end{pmatrix}, \ \alpha \in \mathbb{C}.$$

Then, we obtain

$$\begin{aligned} \tfrac{1}{2} g_2^1(z, 0, \mu) &= \tfrac{1}{2} \mathrm{Proj}_{\mathrm{Ker}(M_2^1)} f_2^1(z, 0, \mu) \\ &= \begin{pmatrix} \mathcal{H}\left((B_{11}\mu_1 + B_{21}\mu_2) z_1\right) \\ \left(B_{13}\mu_1 + B_{23}\mu_2\right) z_3 \end{pmatrix}, \end{aligned} \tag{2.20}$$

where

$$B_{11}=\eta_0^T L_1^{(1,0)}\left(\xi_0 e^{i\omega_c\theta}\right),\ B_{21}=\eta_0^T L_1^{(0,1)}\left(\xi_0 e^{i\omega_c\theta}\right),$$

$$B_{13}=\eta_{k_*}^T L_1^{(1,0)}\left(\xi_{k_*}\right),\ B_{23}=\eta_{k_*}^T\left(L_1^{(0,1)}\left(\xi_{k_*}\right)-\left(\frac{k_*}{\ell}\right)^2 I_d\xi_{k_*}\right),$$

where $I_d=\operatorname{diag}\{d_1,d_2,\cdots,d_n\}$.

2.2. Calculation of $g_3^1(z,0,\varepsilon)$

Since $F(0,\mu)=0$ and $DF(0,\mu)=0$, $F_2(\Phi(\theta)z_x+w,\mu)$ can be written as

$$\begin{aligned}&F_2(\Phi(\theta)z_x+w,\mu)=F_2(\Phi(\theta)z_x+w,0)\\=&\sum_{q_1+q_2+q_3=2}A_{q_1q_2q_3}\gamma_0^{q_1+q_2}(x)\gamma_{k_*}^{q_3}(x)z_1^{q_1}z_2^{q_2}z_3^{q_3}+\mathcal{S}_2\left(\Phi(\theta)z_x,w\right)+O(|w|^2),\end{aligned}\tag{2.21}$$

where S_2 are product terms of $\Phi(\theta)z_x$ and w, $q_1,q_2,q_3\in\mathbb{N}_0$ and

$$A_{q_1q_2q_3}\in\mathbb{C}^n,\ A_{q_1q_2q_3}=\overline{A_{q_2q_1q_3}},$$

we have

$$g_3^1(z,0,\varepsilon)=\operatorname{Proj}_{\operatorname{Ker}(M_3^1)}\widetilde{f_3^1}(z,0,\varepsilon)=Proj_S\widetilde{f_3^1}(z,0,0)+O\left(|z||\varepsilon|^2+|z|^2|\varepsilon|\right),$$

where

$$\begin{aligned}S=&span\left\{z_1^2z_2e_1,z_1z_3^2e_1,z_1z_2^2e_2,z_2z_3^2e_2,z_1z_2z_3e_3,z_3^3e_3\right\},\\ \tilde{f}_3^1(z,0,0)=&f_3^1(z,0,0)+\frac{3}{2}\Big[\left(D_zf_2^1\right)(z,0,0)U_2^1(z,0)\\&+\left(D_wf_2^1\right)(z,0,0)U_2^2(z,0)-\left(D_zU_2^1(z,0)\right)g_2^1(z,0,0)\Big],\end{aligned}$$

with

$$U_2^1(z,0)=\left(M_2^1\right)^{-1}\operatorname{Proj}_{\operatorname{Im}(M_2^1)}f_2^1(z,0,0)\tag{2.22}$$

and

$$\left(M_2^2U_2^2\right)(z,0)=f_2^2(z,0,0).\tag{2.23}$$

Here, the definitions of the operators M_2^1 and M_2^2 are the same as in [8]. We calculate $\operatorname{Proj}_S\tilde{f}_3^1(z,0,0)$ in the following three subsections.

2.2.1. The calculation of $\operatorname{Proj}_S f_3^1(z,0,0)$.

Writing $F_3(\Phi(\theta)z_x,0)$ as follows

$$F_3(\Phi(\theta)z_x,0)=\sum_{q_1+q_2+q_3=3}A_{q_1q_2q_3}\gamma_0^{q_1+q_2}(x)\gamma_{k_*}^{q_3}(x)z_1^{q_1}z_2^{q_2}z_3^{q_3},\ A_{q_1q_2q_3}=\overline{A_{q_2q_1q_3}},\tag{2.24}$$

we have

$$\frac{1}{3!}\operatorname{Proj}_S f_3^1(z,0,0)=\begin{pmatrix}\mathcal{H}\left(C_{210}z_1^2z_2+C_{102}z_1z_3^2\right)\\ C_{111}z_1z_2z_3+C_{003}z_3^3\end{pmatrix},\tag{2.25}$$

where

$$C_{210} = \tfrac{1}{6\ell\pi}\eta_0^T A_{210},\ C_{102} = \tfrac{1}{6\ell\pi}\eta_0^T A_{102},$$
$$C_{111} = \tfrac{1}{6\ell\pi}\eta_{k_*}^T A_{111},\ C_{003} = \tfrac{1}{4\ell\pi}\eta_{k_*}^T A_{003}. \tag{2.26}$$

2.2.2. The calculation of $\mathrm{Proj}_S\left(D_z f_2^1\right)(z,0,0)U_2^1(z,0)$ **and** $\mathrm{Proj}_S\left(D_z U_2^1(z,0)\right) g_2^1(z,0,0)$**.**

$$\frac{1}{3!}\mathrm{Proj}_S\left(D_z f_2^1(z,0,0)U_2^1(z,0)\right) = \begin{pmatrix} \mathcal{H}\left(D_{210}z_1^2 z_2 + D_{102}z_1 z_3^2\right) \\ D_{111}z_1 z_2 z_3 + D_{003}z_3^3 \end{pmatrix}, \tag{2.27}$$

where

$$\begin{aligned} D_{210} &= \tfrac{1}{6\ell\pi\omega_c i}\left\{-\left(\eta_0^T A_{200}\right)\left(\eta_0^T A_{110}\right) + \left|\eta_0^T A_{110}\right|^2 + \tfrac{2}{3}\left|\eta_0^T A_{020}\right|^2\right\}, \\ D_{102} &= \tfrac{1}{6\ell\pi\omega_c i}\left\{-2\left(\eta_0^T A_{200}\right)\left(\eta_0^T A_{002}\right) + \left(\eta_0^T A_{110}\right)\left(\overline{\eta}_0^T A_{002}\right)\right. \\ &\qquad \left. +2\left(\eta_0^T A_{002}\right)\left(\eta_{k_*}^T A_{101}\right)\right\}, \\ D_{111} &= -\tfrac{1}{3\ell\pi\omega_c}\mathrm{Im}\left\{\left(\eta_{k_*}^T A_{101}\right)\left(\eta_0^T A_{110}\right)\right\}, \\ D_{003} &= -\tfrac{1}{3\ell\pi\omega_c}\mathrm{Im}\left\{\left(\eta_{k_*}^T A_{101}\right)\left(\eta_0^T A_{002}\right)\right\}. \end{aligned} \tag{2.28}$$

Note that

$$\frac{1}{3!}\mathrm{Proj}_S\left(D_z U_2^1(z,0)\right) g_2^1(z,0,0) = \begin{pmatrix} 0 & 0 & 0 \end{pmatrix}^T.$$

2.2.3. The calculation of $\mathrm{Proj}_S\left(D_w f_2^1\right)(z,0,0)U_2^2(z,0)$**.**

Let

$$U_2^2(z,0)(\theta) \triangleq h(z) = \sum_{k\geq 0}\sum_{j=1}^{n} h_k^{(j)}(z,\theta)\beta_k^{(j)}$$

with $h_k^{(j)}(z,\theta) = \sum\limits_{q_1+q_2+q_3=2} h_{kq_1q_2q_3}^{(j)}(\theta) z_1^{q_1} z_2^{q_2} z_3^{q_3}$. For simplification of notations, set

$$h_k(z,\theta) = \left(h_k^{(1)}(z,\theta), h_k^{(2)}(z,\theta), \cdots, h_k^{(n)}(z,\theta)\right)^T,\ h_{kq_1q_2q_3}(\theta) = \left(h_{kq_1q_2q_3}^{(1)}(\theta), \cdots, h_{kq_1q_2q_3}^{(n)}(\theta)\right)^T$$

and

$$h_{kq_1q_2q_3}(z,\theta) = h_{kq_1q_2q_3}(\theta) z_1^{q_1} z_2^{q_2} z_3^{q_3}.$$

Then, we have

$$\frac{1}{3!}\mathrm{Proj}_S\left(D_w f_2^1(z,0,0)U_2^2(z,0)\right) = \begin{pmatrix} \mathcal{H}\left(E_{210}z_1^2 z_2 + E_{102}z_1 z_3^2\right) \\ E_{111}z_1 z_2 z_3 + E_{003}z_3^3 \end{pmatrix}, \tag{2.29}$$

where

$$\begin{aligned}
E_{210} &= \tfrac{1}{6\sqrt{\ell\pi}}\eta_0^T\left\{\mathcal{S}_2(\xi_0 e^{i\omega_c\theta}, h_{0110}(\theta)) + \mathcal{S}_2(\overline{\xi}_0 e^{-i\omega_c\theta}, h_{0200}(\theta))\right\},\\
E_{102} &= \tfrac{1}{6\sqrt{\ell\pi}}\eta_0^T\left\{\mathcal{S}_2(\xi_0 e^{i\omega_c\theta}, h_{0002}(\theta)) + \mathcal{S}_2(\xi_{k_*}, h_{k_*101}(\theta))\right\},\\
E_{111} &= \tfrac{1}{6\sqrt{\ell\pi}}\eta_{k_*}^T\left\{\mathcal{S}_2(\xi_0 e^{i\omega_c\theta}, h_{k_*011}(\theta)) + \mathcal{S}_2(\overline{\xi}_0 e^{-i\omega_c\theta}, h_{k_*101}(\theta)) + \mathcal{S}_2(\xi_{k_*}, h_{0110}(\theta))\right\}\\
&\quad + \tfrac{1}{6\sqrt{2\ell\pi}}\eta_{k_*}^T\mathcal{S}_2(\xi_{k_*}, h_{(2k_*)110}(\theta)),\\
E_{003} &= \tfrac{1}{6\sqrt{\ell\pi}}\eta_{k_*}^T\mathcal{S}_2(\xi_{k_*}, h_{0002}(\theta)) + \tfrac{1}{6\sqrt{2\ell\pi}}\eta_{k_*}^T\mathcal{S}_2(\xi_{k_*}, h_{(2k_*)002}(\theta)).
\end{aligned} \tag{2.30}$$

Clearly, we still need to compute h_{0110}, h_{0200}, h_{0002}, h_{k_*101}, h_{k_*011}, $h_{(2k_*)110}$, $h_{(2k_*)002}$. From [8] and (2.15), defining $X_0(\theta) = 0$ for $-1 \le \theta < 0$ and $X_0(0) = 0$, then we have

$$\begin{aligned}
&M_2^2\left(\sum_{j=1}^{n} h_k^{(j)}(z,\theta)\beta_k^{(j)}\right)\\
&= \left(D_z\left(\sum_{j=1}^{n} h_k^{(j)}(z,\theta)\beta_k^{(j)}\right)Bz\right) - A_{\mathscr{Q}^1}\left(\sum_{j=1}^{n} h_k^{(j)}(z,\theta)\beta_k^{(j)}\right),
\end{aligned}$$

which leads to

$$\begin{aligned}
&\begin{pmatrix}
\left[M_2^2\left(\sum_{j=1}^{n} h_k^{(j)}(z,\theta)\beta_k^{(j)}\right), \beta_k^{(1)}\right]\\
\cdots\\
\left[M_2^2\left(\sum_{j=1}^{n} h_k^{(j)}(z,\theta)\beta_k^{(j)}\right), \beta_k^{(n)}\right]
\end{pmatrix}\\
&= i\omega_c\left(2h_{k200}(\theta)z_1^2 + h_{k101}(\theta)z_1z_3 - 2h_{k020}(\theta)z_2^2 - h_{k011}(\theta)z_2z_3\right)\\
&\quad -\left(\dot{h}_k(z,\theta) + X_0(\theta)\left[L_0(h_k(z,\theta)) + \tau_*\mathrm{diag}\left\{\delta_k^{(1)}, \delta_k^{(2)}, \cdots, \delta_k^{(n)}\right\}h_k(z,0) - \dot{h}_k(z,0)\right]\right).
\end{aligned} \tag{2.31}$$

By (2.14), we get

$$\begin{aligned}
f_2^2(z,0,0) &= (I-\pi)X_0(\theta)\widetilde{F}_2\left(\Phi(\theta)z_x, 0\right)\\
&= X_0(\theta)\widetilde{F}_2\left(\Phi(\theta)z_x, 0\right) - \Phi_1(\theta)\Psi_1(0)\begin{pmatrix}
\left[\widetilde{F}_2\left(\Phi(\theta)z_x, 0\right), \beta_0^{(1)}\right]\\
\cdots\\
\left[F_2\left(\Phi(\theta)z_x, 0\right), \beta_0^{(n)}\right]
\end{pmatrix}\gamma_0(x)\\
&\quad -\Phi_2(\theta)\Psi_2(0)\begin{pmatrix}
\left[\widetilde{F}_2\left(\Phi(\theta)z_x, 0\right), \beta_{k_*}^{(1)}\right]\\
\cdots\\
\left[F_2\left(\Phi(\theta)z_x, 0\right), \beta_{k_*}^{(n)}\right]
\end{pmatrix}\gamma_{k_*}(x).
\end{aligned}$$

So,

$$\begin{pmatrix} \left[f_2^2(z,0,0),\beta_k^{(1)}\right] \\ \cdots \\ \left[f_2^2(z,0,0),\beta_k^{(n)}\right] \end{pmatrix} = \begin{cases} \frac{1}{\sqrt{\ell\pi}}\left(X_0(\theta)-\Phi_1(\theta)\Psi_1(0)\right)\left(A_{200}z_1^2+A_{020}z_2^2\right. & k=0, \\ \left.+A_{002}z_3^2+A_{110}z_1z_2\right), & \\ \frac{1}{\sqrt{\ell\pi}}\left(X_0(\theta)-\Phi_2(\theta)\Psi_2(0)\right)\left(A_{101}z_1z_3+A_{011}z_2z_3\right), & k=k_*, \\ \frac{1}{\sqrt{2\ell\pi}}X_0(\theta)A_{002}z_3^2, & k=2k_*. \end{cases} \tag{2.32}$$

Hence, denote

$$\mathscr{L}_k\left(h(\theta)\right) = L_0\left(h(\theta)\right) + \tau_*\mathrm{diag}\left\{\delta_k^{(1)},\delta_k^{(2)},\cdots,\delta_k^{(n)}\right\}\left(h(\theta)\right)$$

and then from (2.31), (2.32) and matching the coefficients of $z_1^2, z_1z_2, z_1z_3, z_2z_3, z_3^2$, we have

$$k=0,\quad \begin{cases} z_1^2: & \begin{cases} \dot{h}_{0200}(\theta) - 2i\omega_c h_{0200}(\theta) = \frac{1}{\sqrt{\ell\pi}}\Phi_1(\theta)\Psi_1(0)A_{200}, \\ \dot{h}_{0200}(0) - \mathscr{L}_0(h_{0200}(\theta)) = \frac{1}{\sqrt{\ell\pi}}A_{200}, \end{cases} \\ z_1z_2: & \begin{cases} \dot{h}_{0110}(\theta) = \frac{1}{\sqrt{\ell\pi}}\Phi_1(\theta)\Psi_1(0)A_{110}, \\ \dot{h}_{0110}(0) - \mathscr{L}_0(h_{0110}(\theta)) = \frac{1}{\sqrt{\ell\pi}}A_{110}, \end{cases} \\ z_3^2: & \begin{cases} \dot{h}_{0002}(\theta) = \frac{1}{\sqrt{\ell\pi}}\Phi_1(\theta)\Psi_1(0)A_{002}, \\ \dot{h}_{0002}(0) - \mathscr{L}_0\left(h_{0002}(\theta)\right) = \frac{1}{\sqrt{\ell\pi}}A_{002}, \end{cases} \end{cases} \tag{2.33}$$

$$k=k_*,\ z_1z_3: \begin{cases} \dot{h}_{k_*101}(\theta) - i\omega_c h_{k_*101}(\theta) = \frac{1}{\sqrt{\ell\pi}}\Phi_2(\theta)\Psi_2(0)A_{101}, \\ \dot{h}_{k_*101}(0) - \mathscr{L}_{k_*}h_{k_*101}(0) = \frac{1}{\sqrt{\ell\pi}}A_{101}, \end{cases} \tag{2.34}$$

$$k=2k_*, \begin{cases} z_3^2: & \begin{cases} \dot{h}_{(2k_*)002}(\theta) = \mathbf{0}, \\ \dot{h}_{(2k_*)002}(0) - \mathscr{L}_{2k_*}\left(h_{(2k_*)002}(0)\right) = \frac{1}{\sqrt{2\ell\pi}}A_{002}, \end{cases} \\ z_1z_2: & \begin{cases} \dot{h}_{(2k_*)110}(\theta) = \mathbf{0}, \\ \dot{h}_{(2k_*)110}(0) - \mathscr{L}_{2k_*}\left(h_{(2k_*)110}(0)\right) = \mathbf{0}, \end{cases} \end{cases} \tag{2.35}$$

and $h_{k^*011} = \overline{h}_{k^*101}$.

Let

$$B_{210} = C_{210} + \frac{3}{2}\left(D_{210}+E_{210}\right),\ B_{102} = C_{102} + \frac{3}{2}\left(D_{102}+E_{102}\right),$$
$$B_{111} = C_{111} + \frac{3}{2}\left(D_{111}+E_{111}\right),\ B_{003} = C_{003} + \frac{3}{2}\left(D_{003}+E_{003}\right).$$

Then, by (2.20),(2.25), (2.27) and (2.29), and transforming the system (2.16) to the cylindrical coordinates form, we obtain the normal form truncated to the third order terms for the Turing-Hopf bifurcation as follows

$$\begin{cases} \dot{\rho} = \alpha_1(\mu)\rho + \kappa_{11}\rho^3 + \kappa_{12}\rho r^2, \\ \dot{r} = \alpha_2(\mu)r + \kappa_{21}\rho^2 r + \kappa_{22}r^3, \end{cases} \tag{2.36}$$

where

$$\alpha_1(\mu) = \mathrm{Re}\,(B_{11})\,\mu_1 + \mathrm{Re}\,(B_{21})\,\mu_2,\ \alpha_2(\mu) = \mathrm{Re}\,(B_{13})\,\mu_1 + \mathrm{Re}\,(B_{23})\,\mu_2,$$
$$\kappa_{11} = \mathrm{Re}\,(B_{210})\,,\ \kappa_{12} = \mathrm{Re}\,(B_{102})\,,\ \kappa_{21} = B_{111},\ \kappa_{22} = B_{003}.$$

3. The dynamics of diffusive predator-prey model with weak Allee effect and delay

Using the developed algorithm in the previous section, we consider the following diffusive predator-prey model with weak Allee effect and delay under the Neumann boundary condtion

$$\begin{cases} \frac{\partial u(x,t)}{\partial t} = d_1 u_{xx}(x,t) + u^2(x,t)(1-u(x,t)) - u(x,t)v(x,t-\tau),\ 0<x<\pi, t>0, \\ \frac{\partial v(x,t)}{\partial t} = d_2 v_{xx}(x,t) + \delta v(x,t)\left(1 - \frac{v(x,t)}{\gamma u(x,t)}\right),\ 0<x<\pi, t>0, \\ u_x(0,t) = u_x(\pi,t) = v_x(0,t) = v_x(\pi,t) = 0,\ t \geq 0, \end{cases} \tag{3.1}$$

where $u(x,t)$ and $v(x,t)$ can be interpreted as the densities of prey and predator populations, respectively, d_1 and d_2 are the corresponding coefficients of the diffusion in space, δ stands for the conversion rate of prey into predators biomass and τ represents the hunting delay of the predator species. For the biological meaning of this model, see [4,10,25,43] and references therein.

Clearly, there exists a positive constant steady state $E^*\left(1-\gamma, \gamma(1-\gamma)\right)$ in (3.1) provided that $0<\gamma<1$. Therefore, the linearization of (3.1) at the equilibrium E^* is

$$\begin{pmatrix} \frac{\partial u(x,t)}{\partial t} \\ \frac{\partial v(x,t)}{\partial t} \end{pmatrix} = d\Delta \begin{pmatrix} u(x,t) \\ v(x,t) \end{pmatrix} + A_0 \begin{pmatrix} u(x,t) \\ v(x,t) \end{pmatrix} + A_1 \begin{pmatrix} u(x,t-\tau) \\ v(x,t-\tau) \end{pmatrix} \tag{3.2}$$

with

$$d\Delta = \begin{pmatrix} d_1\Delta & 0 \\ 0 & d_2\Delta \end{pmatrix},\ A_0 = \begin{pmatrix} a_{11} & 0 \\ a_{21} & a_{22} \end{pmatrix},\ A_1 = \begin{pmatrix} 0 & a_{12} \\ 0 & 0 \end{pmatrix},$$

where for $0<\gamma<1$,

$$a_{11} = (1-\gamma)(2\gamma-1)\begin{cases} \leq 0,\ 0<\gamma\leq 1/2, \\ >0,\ 1/2<\gamma<1, \end{cases} \quad a_{12} = \gamma - 1 < 0,$$
$$a_{21} = \delta\gamma > 0,\ a_{22} = -\delta < 0. \tag{3.3}$$

The characteristic equation of (3.2) is (2.2) with

$$\Gamma_k = \lambda^2 + T_k\lambda + D_k(\tau) = 0,\ k \in \mathbb{N}_0, \tag{3.4}$$

where

$$T_k = \left((d_1+d_2)\,k^2 - (a_{11}+a_{22})\right) = (d_1+d_2)\,k^2 + \delta - (1-\gamma)(2\gamma-1), \tag{3.5}$$

and

$$
\begin{aligned}
&D_k(\tau)\\
&= d_1d_2k^4 - (d_2a_{11} + d_1a_{22})\,k^2 + a_{11}a_{22} - a_{12}a_{21}e^{-\lambda\tau}\\
&= d_1d_2k^4 + (d_1\delta - d_2(1-\gamma)(2\gamma-1))k^2 - \delta(1-\gamma)(2\gamma-1) + \delta\gamma(1-\gamma)e^{-\lambda\tau}.
\end{aligned}
\tag{3.6}
$$

3.1. Stability and diffusion-driven Turing instability for the case without delay

Without diffusion and delay ($d_1 = d_2 = \tau = 0$), system (3.1) becomes the following ordinary differential model

$$
\begin{cases}
\frac{du(t)}{dt} = u^2(t)(1-u(t)) - u(t)v(t),\\
\frac{dv(t)}{dt} = \delta v(t)\left(1 - \frac{v(t)}{\gamma u(t)}\right).
\end{cases}
\tag{3.7}
$$

Clearly, the system (3.1) and (3.7) have the same positive equilibrium E^*. By a simple linear analysis, we can obtian the following result.

Lemma 3.1. *For system* (3.7) *with* $0 < \gamma < 1$, *the positive equilibrium* E^* *is stable when* $(\gamma, \delta) \in R_1$ *and unstable when* $(\gamma, \delta) \in R_2$, *and* H_0 *is the Hopf bifurcation curve, where*

$$
R_1 = \left\{(\gamma,\delta)\,\middle|\, 0 < \gamma \le \frac{1}{2},\ \delta > 0\right\} \cup \left\{(\gamma,\delta)\,\middle|\, \frac{1}{2} < \gamma < 1, \delta > (1-\gamma)(2\gamma-1)\right\},
$$

$$
R_2 = \left\{(\gamma,\delta)\,\middle|\, \frac{1}{2} < \gamma < 1,\ 0 < \delta < (1-\gamma)(2\gamma-1)\right\}.
$$

and H_0 *is defined by*

$$
H_0:\ \delta = (1-\gamma)(2\gamma-1),\ \frac{1}{2} < \gamma < 1. \tag{3.8}
$$

Next, we investigate the effect of diffusion on the positive equilibrium E^* of (3.1) in the case of $\tau = 0$. For convenient statement, we rewrite system (3.1) with $\tau = 0$ as

$$
\begin{cases}
\frac{\partial u(x,t)}{\partial t} = d_1u_{xx}(x,t) + u^2(x,t)(1-u(x,t)) - u(x,t)v(x,t),\ 0 < x < \pi, t > 0,\\
\frac{\partial v(x,t)}{\partial t} = d_2v_{xx}(x,t) + \delta v(x,t)\left(1 - \frac{v(x,t)}{\gamma u(x,t)}\right),\ 0 < x < \pi, t > 0,\\
u_x(0,t) = u_x(\pi,t) = v_x(0,t) = v_x(\pi,t) = 0,\ t \ge 0.
\end{cases}
\tag{3.9}
$$

Then, we have the following Theorem.

Theorem 3.1. *For the positive equilibrium* E^* *of system* (3.9), *when* $0 < \gamma < 1$, *we have the following results on its stability and Turing instability.*

(i) When $0 < d_2 \le d_1$, *there is no diffusion-driven Turing instability, and the stability region is exactly the same to the case without diffusion.*

(ii) When $0 < d_1 < d_2$, Turing instability may occur for

$$(1-\gamma)(2\gamma-1) < \delta < \beta(1-\gamma)(2\gamma-1) - 2(1-\gamma)\sqrt{\beta\delta}, \ \gamma_h < \gamma < 1, \tag{3.10}$$

where $\beta = d_2/d_1$ and $\gamma_h = \frac{1}{2} + \frac{\beta}{1+\beta^2}$.

Proof. (i) By the characteristic equation (3.4), the positive equilibrium E^* of system (3.9) is locally stable if and only if $T_k > 0, D_k(0) > 0$ for all $k \in \mathbb{N}_0$.

Firstly, we have

$$D_0(0) = \delta(1-\gamma)^2 > 0, \ T_0 = \delta - (1-\gamma)(2\gamma-1).$$

When $0 < d_2 \leq d_1$ and $(\gamma, \delta) \in R_1$, it is easy to verify $(d_1\delta - d_2(1-\gamma)(2\gamma-1)) > 0$, which implies that $D_k(0) = d_1 d_2 k^4 + (d_1\delta - d_2(1-\gamma)(2\gamma-1))k^2 + D_0(0) > 0$. In addition, $T_0 = \delta - (1-\gamma)(2\gamma-1) > 0$ if and only if $(\gamma, \delta) \in R_1$ and $T_k > 0$ provided that $T_0 > 0$. The conclusion (i) is confirmed.

(ii) Assume that $T_0 > 0$ and $D_0(0) > 0$, i.e., the positive equilibrium is stable without diffusion. We investigated the effect of the diffusion on the stability of the positive equilibrium. Notcing that if $T_0 > 0$, then $T_k = (d_1+d_2)k^2 + T_0 > 0$. Thus, the necessary condition for the occurrence of Turing instability is $d_1 a_{22} + d_2 a_{11} > 0$ and $4d_1 d_2 (a_{11}a_{22} - a_{12}a_{21}) - (d_1 a_{22} + d_2 a_{11})^2 < 0$. By (3.3), it is easy to verify that the inequality $d_1 a_{22} + d_2 a_{11} > 0$ is equivalent to $\delta < \beta(1-\gamma)(2\gamma-1)$ and the inequality $4d_1 d_2 (a_{11}a_{22} - a_{12}a_{21}) - (d_1 a_{22} + d_2 a_{11})^2 < 0$ is equivalent to

$$0 < \delta < \beta(1-\gamma)(2\gamma-1) - 2(1-\gamma)\sqrt{\beta\delta}. \tag{3.11}$$

In the $\gamma - \delta$ plane, define a curve L by

$$L: \ \delta = \beta(1-\gamma)(2\gamma-1) - 2(1-\gamma)\sqrt{\beta\delta}. \tag{3.12}$$

It is easy to verify that the curves L and H_0 intersect at $\gamma = \gamma_h$. Taking δ as a parameter and letting $\lambda(\delta)$ be the root of Eq.(3.4) with $\tau = 0$ near $\delta = \delta_*$ satisfying $\lambda(\delta_*) = 0$. Differentiating the two sides of Eq. (3.4) with respect to δ, we obtain

$$\left.\frac{d\lambda(\delta)}{d\delta}\right|_{\delta=\delta_*} = -\frac{(1-\gamma)^2 + d_1 k^2}{(d_1+d_2)k^2 + \delta_* - (1-\gamma)(2\gamma-1)} < 0.$$

In addition, noticing that the stability region is R_1 in the absence of diffusion. Thus, the proof of conclusion (ii) is completed. □

Notice that the condition (3.10) is not the sufficient and necessary condition for the occurrence of Turing instability since the critical wave number should be positive integer under the Neumann boundary condition. And the curve L defined by (3.12) is not the exact boundary between the stability region and Turing instability region. In what follows, we seek the exact boundary of Turing instability for the case $0 < d_1 < d_2$.

Theorem 3.2. *For system (3.9), assume that $0 < \gamma < 1$ and $0 < d_1 < d_2$. Let $\delta = \delta(\gamma)$ be the function defined by the implicit function $\delta = \beta(1-\gamma)(2\gamma-1) - 2(1-\gamma)\sqrt{\beta\delta}$ and define*

$$\gamma_k = \frac{3+\sqrt{7}}{8}, \ \beta_c = \frac{\sqrt{7}+5}{\sqrt{7}-1}, \ \delta_h = \delta(\gamma_h), \ \delta_k = \delta(\gamma_k),$$

and

$$\tilde{k}_c = \left[k_c^M\right], \tag{3.13}$$

where $[\cdot]$ *is the integer function and* k_c^M *is defined by* (3.16). *Then we have the following:*

(*i*) *When* $\tilde{k}_c < 1$*, there is no diffusion-driven Turing instability and the positive equilibrium* E^* *is stable when* $(\gamma, \delta) \in R_1$*;*

(*ii*) *When* $\tilde{k}_c \geq 1$*, Turing instability occurs for* $(\gamma, \delta) \in R_{12}$*, where the region* R_{12} *is surrounded by the Hopf bifurcation curve* H_0 *and Turing bifurcation curves* L_k *with* $k = 1, \cdots, \tilde{k}_c$*; the positive equilibrium* E^* *is stable for* $(\gamma, \delta) \in R_{11}$ *and unstable for* $(\gamma, \delta) \in R_2 \cup R_{12}$*, where* $R_{11} = R_1 \setminus R_{12}$*, and* L_k *is defined by*

$$L_k: \ \delta = \frac{-d_1 d_2 k^4 + d_2(1-\gamma)(2\gamma - 1)k^2}{d_1 k^2 + (1-\gamma)^2}. \tag{3.14}$$

Proof. On the curve L defined by (3.12) , the critical wave number k_c is determined by

$$k_c^2 = \frac{-\delta + \beta(1-\gamma)(2\gamma-1)}{2d_2} = \frac{(1-\gamma)\sqrt{\beta\delta}}{d_2}. \tag{3.15}$$

Then L_k defined by (3.14) is followed from $D_k(0) = 0$. It is easy to verify that the curves L and H_0 intersect at $\gamma = \gamma_h$. Thus, if there exists at least one positive integer k such that for $\gamma_h \leq \gamma < 1$, the curve L_k is tangent to L, then Turing instability occurs.

By (3.15), letting $Z(\gamma) = \frac{(1-\gamma)\sqrt{\beta\delta}}{d_2}$, we have

$$Z'(\gamma) = \frac{\sqrt{\beta\delta}}{2d_2\delta}\left(-2\delta + (1-\gamma)\delta'(\gamma)\right) \begin{cases} > 0, \ \delta < \frac{\beta}{2}(1-\gamma)(-4\gamma+3), \\ = 0, \ \delta = \frac{\beta}{2}(1-\gamma)(-4\gamma+3), \\ < 0, \ \delta > \frac{\beta}{2}(1-\gamma)(-4\gamma+3). \end{cases}$$

Solving $\delta = \frac{\beta}{2}(1-\gamma)(-4\gamma+3)$ and $\delta = \beta(1-\gamma)(2\gamma-1) - 2(1-\gamma)\sqrt{\beta\delta}$, we have $\gamma = \gamma_k$. Thus, on the curve L, the critical wave number k_c is increasing with γ for $0 < \gamma < \gamma_k$ and decreasing with γ for $\gamma > \gamma_k$. Solving $\gamma_h = \gamma_k$ yields to $\beta = \beta_c$. And $\gamma_k \leq \gamma_h$ for $\beta \leq \beta_c$ and $\gamma_k > \gamma_h$ for $\beta > \beta_c$. Thus, define

$$k_c^M = \begin{cases} \sqrt{\frac{(1-\gamma_h)\sqrt{\beta\delta_h}}{d_2}}, \ 1 < \beta \leq \beta_c, \\ \sqrt{\frac{(1-\gamma_k)\sqrt{\beta\delta_k}}{d_2}}, \ \beta > \beta_c. \end{cases} \tag{3.16}$$

Then, for $\gamma_h \leq \gamma < 1$, the critical wave number k_c satisfies $0 < k_c < k_c^M$. Therefore, let $\tilde{k}_c = \left[k_c^M\right]$. Then, if $\tilde{k}_c < 1$, then for $\gamma_h \leq \gamma < 1$, there is no Turing bifurcation curve L_k. In this case, there is no diffusion-driven Turing instability.

If $\tilde{k}_c \geq 1$, there are $\tilde{k}_c$ Turing bifurcation curves L_k tangent to the curve L for $\gamma_h \leq \gamma < 1$, and the boundaries of Turing instability region consist of these curves L_k with $k = 1, \cdots, \tilde{k}_c$. The proof is completed. □

According to Lemma 3.1 and Theorems 3.1, for $0 < d_2 \leq d_1$, there is no diffusion-driven Turing instability for system (3.9), the stability and instability regions are

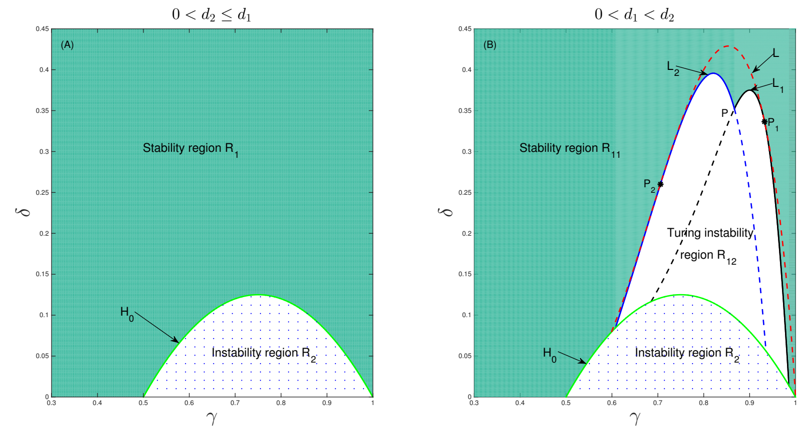

Figure 1. Stability and Turing instability regions for system (3.9). (A): when $0 < d_2 \le d_1$, there is no Turing instability and the shaded region R_1 is the stability region of the positive equilibrium E^* ; (B): when $0 < d_1 < d_2$, Turing instability region is the white region R_{12} and the shaded region R_{11} is the stability region of the positive equilibrium E^*. Here $d_1 = 0.0125, d_2 = 0.125$.

illustrated in Fig.1(A). When $d_2 > d_1$, Turing instability may occur. Letting $\delta = \delta(\gamma)$ be the function defined by (3.12). From

$$\delta'(\gamma) = \frac{\delta(\beta(-4\gamma+3) + 2\sqrt{\beta\delta})}{\delta + (1-\gamma)\sqrt{\beta\delta}} \begin{cases} > 0, \, \gamma < \gamma_c, \\ = 0, \, \gamma = \gamma_c, \\ < 0, \, \gamma > \gamma_c, \end{cases}$$

where $\gamma_c = \frac{3+2\sqrt{2}}{4+2\sqrt{2}}$, obviously, the function $\delta(\gamma)$ is increasing for $\gamma < \gamma_c$ and decreasing for $\gamma > \gamma_c$. Taking $d_1 = 0.0125, d_2 = 0.125$, implying $\beta = 10 > \beta_c = \left(\sqrt{7}+5\right)/\left(\sqrt{7}-1\right)$, then $\tilde{k}_c = 2$ follows from Theorem 3.2 and (3.13) . Thus, there are only two Turing bifurcation curves L_1 and L_2 tangent to the curve L for $\gamma_h \le \gamma < 1$. Numerical calculation confirms that these two Turing bifurcation curves L_1 and L_2 intersect at $P(0.8668, 0.3522)$ and are tangent to the curve L, respectively, at $P_1(0.9325, 0.3362)$ and $P_2(0.7, 0.25)$ (Fig.1(B)). In Fig.1(B), the stability region for the positive equilibrium E^* is marked by R_{11}, the region R_{12} (the white region) is diffusion-driven Turing instability region which is surround by the Turing bifurcation curves L_1 and L_2 (the solid line) and the Hopf bifurcation curve H_0. The positive equilibrium E^* is stable for $(\gamma, \delta) \in R_{11}$ and unstable for $(\gamma, \delta) \in R_{12} \cup R_2$.

3.2. Delay-induced Hopf bifurcation and Turing-Hopf bifurcation

In this section, we investigate the effect of the delay on the stability of the positive equilibrium E^* of system (3.9) and delay-induced bifurcation phenomenon. We focus on the following two cases:

Case (i) either $0 < d_2 \le d_1$ and $(\gamma, \delta) \in R_1$, or $0 < d_1 < d_2$ and $(\gamma, \delta) \in R_{11}$;

Case (ii) $0 < d_1 < d_2$ and (γ, δ) lies on L_k with $k \in \mathbb{N}$ and $0 < k \le \tilde{k}_c$.

When $\tau = 0$, we know that the positive equilibrium E^* of (3.9) is stable for case (i) and the parameter pair (γ, δ) lies on the boundary of Turing instability region for case (ii).

In what follows, for simplication of notations, we denote by k_* for some k satisfying $k \in \mathbb{N}$ and $0 < k \le \tilde{k}_c$ and the corresponding Turing bifurcation curve is L_{k_*}.

From Theorems 3.1 and 3.2, we first have the following results on the distribution of roots of the characteristic equation (3.4) when $\tau = 0$.

Lemma 3.2. *For $\tau = 0$, we have the following:*

(i) For case (i), all roots of Eq.(3.4) have negative real parts;

(ii) For case (ii), Eq.(3.4) has a simple zero root $\lambda = 0$ when $k = k_*$, no root with zero real parts when $k \in \mathbb{N}_0$ and $k \ne k_*$.

When $\tau > 0$, the following theorem describes the distribution of roots of the characteristic equation (3.4).

Lemma 3.3. *Assume that ω_k and $\tau_{k,j}$ are defined by (3.24) and (3.27), respectively and*

$$k_c^* = \begin{cases} k_0 - 1, \; k_0 \in \mathbb{N}, \\ \\ \;[k_0], \quad k_0 \notin \mathbb{N}, \end{cases} \tag{3.17}$$

where $[\cdot]$ is the integer function and k_0 is the unique positive root of $\tilde{Q}_k$ given in (3.23) . We have the following:

(i) when $0 < \gamma \le \frac{1}{3}$, Eq.(3.4) has no purely imaginary roots;

(ii) when $\frac{1}{3} < \gamma < 1$, for case (i), Eq.(3.4) has a pair of purely imaginary roots $\pm i\omega_k$ at $\tau = \tau_{k,j}$, $k \in \{0, 1, \cdots, k_c^*\}, j \in \mathbb{N}_0$, no purely imaginary roots for any $\tau \ge 0$ when $k \ge k_c^* + 1$;

(iii) For case (ii), Eq.(3.4) has a pair of purely imaginary roots $\pm i\omega_k$ at $\tau = \tau_{k,j}$, $k \in \{0, 1, \cdots, k_c^*\}, j \in \mathbb{N}_0$, and $k \ne k_*$, no purely imaginary roots for any $\tau \ge 0$ when either $k = k_*$ or $k \ge k_c^* + 1$.

Proof. Assume that $i\omega (\omega > 0)$ is a root of (3.4), then we have

$$\begin{aligned} &\omega^2 - \big((d_1 + d_2)\, k^2 - (a_{11} + a_{22})\big)\, \omega i - d_1 d_2 k^4 + (d_2 a_{11} + d_1 a_{22})\, k^2 \\ &- a_{11} a_{22} + a_{12} a_{21} (\cos \omega\tau - i \sin \omega\tau) = 0. \end{aligned} \tag{3.18}$$

Separating the real and imaginary parts of (3.18) leads to

$$\begin{cases} \omega^2 - \big(d_1 d_2 k^4 - (d_2 a_{11} + d_1 a_{22})\, k^2 + a_{11} a_{22}\big) + a_{12} a_{21} \cos \omega\tau = 0, \\ \big((d_1 + d_2)\, k^2 - (a_{11} + a_{22})\big)\, \omega + a_{12} a_{21} \sin \omega\tau = 0. \end{cases} \tag{3.19}$$

By (3.19), we have

$$\omega^4 + P_k \omega^2 + Q_k = 0, \;\; k \in \mathbb{N}_0 \tag{3.20}$$

with

$$P_k = \left(d_1 k^2 - a_{11}\right)^2 + \left(d_2 k^2 - a_{22}\right)^2 > 0, \tag{3.21}$$

$$Q_k = \left(d_1 d_2 k^4 - \left(d_1 a_{22} + d_2 a_{11}\right) k^2 + a_{11} a_{22}\right)^2 - \left(a_{12} a_{21}\right)^2 = D_k(0) \cdot \tilde{Q}_k, \tag{3.22}$$

where

$$D_k(0) = d_1 d_2 k^4 - \left(d_1 a_{22} + d_2 a_{11}\right) k^2 + a_{11} a_{22} - a_{12} a_{21}$$

and

$$\tilde{Q}_k = d_1 d_2 k^4 - \left(d_1 a_{22} + d_2 a_{11}\right) k^2 + a_{11} a_{22} + a_{12} a_{21}. \tag{3.23}$$

Then, by a simple analysis, we have $D_k(0) > 0$ and $\tilde{Q}_k > 0$ for $0 < \gamma \leq \frac{1}{3}$ from (3.3) and

$$\tilde{Q}_0 = a_{11} a_{22} + a_{12} a_{21} = -\delta(1-\gamma)(3\gamma - 1) \begin{cases} \geq 0, \; 0 < \gamma \leq \frac{1}{3}, \\ < 0, \; \frac{1}{3} < \gamma < 1. \end{cases}$$

Therefore, Eq.(3.20) has no positive real roots. This completes the proof of conclusion (i).

It follows from Theorem 3.2 that for case (i) we have $D_k(0) > 0$ for $k \in \mathbb{N}_0$. Notice that $\tilde{Q}_k$ is a quadratic polynomial with respect to k^2 and $\tilde{Q}_0 < 0$ for $\frac{1}{3} < \gamma < 1$. Thus, we can conclude that there exists $k_0 > 0$ such that $\tilde{Q}_{k_0} = 0$ and

$$Q_k = D_k(0) \tilde{Q}_k \begin{cases} < 0, \; 0 \leq k \leq k_c^*, \\ \geq 0, \; k \geq k_c^* + 1, \end{cases} \qquad k \in \mathbb{N}_0,$$

where k_c^* is defined by (3.17). Thus, Eq.(3.20) has only one positive root ω_k for fixed $k \in [0, k_c^*]$ and $k \in \mathbb{N}_0$, where

$$\omega_k^2 = \frac{1}{2}\left(-P_k + \sqrt{P_k^2 - 4Q_k}\right) = \frac{2}{\sqrt{\frac{P_k^2}{(-Q_k)^2} + \frac{4}{-Q_k}} + \frac{P_k}{-Q_k}}. \tag{3.24}$$

But for $k \geq k_c^* + 1$, (3.24) has no positive real root, which implies that Eq.(3.4) has no purely imaginary roots for any $\tau \geq 0$.

By (3.19), we have

$$\cos \omega\tau = \frac{\omega^2 - \left(d_1 k^2 - a_{11}\right)\left(d_2 k^2 - a_{22}\right)}{-a_{12} a_{21}} \tag{3.25}$$

and

$$\sin \omega\tau = \frac{\left(\left(d_1 + d_2\right) k^2 - \left(a_{11} + a_{22}\right)\right)\omega}{-a_{12} a_{21}}. \tag{3.26}$$

It follows from (3.26) that $\sin \omega\tau > 0$ since $-\left(a_{11} + a_{22}\right) = \delta - (1-\gamma)(2\gamma - 1) > 0$ and $a_{12} a_{21} < 0$. Thus, by (3.25), we can define

$$\tau_{k,j} = \frac{1}{\omega_k}\left(\arccos \frac{\omega_k^2 - \left(d_1 k^2 - a_{11}\right)\left(d_2 k^2 - a_{22}\right)}{-a_{12} a_{21}} + 2j\pi\right), \; 0 \leq k \leq k_c^*, \; k, j \in \mathbb{N}_0. \tag{3.27}$$

Then (3.4) has a pair of purely imaginary roots $\pm i\omega_k$ at $\tau = \tau_{k,j}$. This confirms conclusion (ii).

When $0 < d_1 < d_2$ and $(\gamma,\delta) \in L_{k_*}$, $D_{k_*}(0) = 0$ and $D_k(0) > 0$ for $k \in \mathbb{N}_0$ and $k \neq k_*$. Since $\tilde{Q}_k = D_k(0) - 2\delta\gamma(1-\gamma)$, we have $\tilde{Q}_{k_*} = D_{k_*}(0) - 2\delta\gamma(1-\gamma) = -2\delta\gamma(1-\gamma) < 0$. Thus, $k_* \leq k_c^*$. Then we have

$$Q_k = D_k(0)\tilde{Q}_k \begin{cases} < 0,\ 0 \leq k \leq k_c^* \text{ and } k \neq k_*, \\ = 0,\ k = k_*, \\ \geq 0,\ k \geq k_c^* + 1, \end{cases}$$

which, together with $P_k > 0$, complets the proof of conclusion (iii). □

If taking τ as a parameter, letting $\lambda(\tau) = \alpha(\tau) + i\beta(\tau)$ be the pair of roots of Eq.(3.4) near $\tau = \tau_{k,j}$ satisfying $\alpha(\tau_{k,j}) = 0$ and $\beta(\tau_{k,j}) = \omega_k$, we have the following transversality condition.

Lemma 3.4. $\left.\frac{d\mathrm{Re}(\lambda(\tau))}{d\tau}\right|_{\tau=\tau_{k,j}} > 0$.

Proof. Differentiating the two sides of Eq. (3.4) with respect to τ, we obtain

$$\left(\frac{d\lambda(\tau)}{d\tau}\right)^{-1} = \frac{(2\lambda + T_k)e^{\lambda\tau}}{-a_{12}a_{21}\lambda} - \frac{\tau}{\lambda}.$$

By (3.4), (3.25) and (3.26), we have

$$\begin{aligned} \mathrm{Re}\left(\left.\frac{d\lambda(\tau)}{d\tau}\right|_{\tau=\tau_{k,j}}\right)^{-1} &= \mathrm{Re}\left(\frac{(2i\omega_k + T_k)e^{i\omega_k\tau_{k,j}}}{-i\omega_k a_{12}a_{21}}\right) \\ &= \mathrm{Re}\left(\frac{(-2\omega_k^2 + i\omega_k T_k)(\cos\omega_k\tau_{k,j} + i\sin\omega_k\tau_{k,j})}{\omega_k^2(a_{12}a_{21})^2}\right) \\ &= \frac{\left(-2\omega_k^2\cos\omega_k\tau_{k,j} - \omega T_k\sin\omega_k\tau_{k,j}\right)a_{12}a_{21}}{\omega_k^2(a_{12}a_{21})^2} \\ &= \frac{2\omega_k^2 + \left(d_1k^2 + a_{11}\right)^2 + \left(d_2k^2 + a_{22}\right)^2}{(a_{12}a_{21})^2} > 0. \end{aligned}$$

This, together with the fact that

$$\mathrm{sgn}\left\{\left.\frac{d\mathrm{Re}(\lambda(\tau))}{d\tau}\right|_{\tau=\tau_{k,j}}\right\} = \mathrm{sgn}\left\{\mathrm{Re}\left(\left.\frac{d\lambda(\tau)}{d\tau}\right|_{\tau=\tau_{k,j}}\right)^{-1}\right\},$$

completes the proof. □

In terms of Lemmas 3.2, 3.3 and 3.4 , we have the following results on stability, Hopf bifurcation and Turing-Hopf bifurcation induced by delay.

Theorem 3.3. *Denote* $\tau_* = \min\{\tau_{k,j}, 0 \leq k \leq k_c^*, j \in \mathbb{N}_0\}$, $\tau_{k,j}$ *are given in* (3.27). E^* *is the positive equilibriumof system* (3.1).

- (i) *When* $0 < \gamma \leq \frac{1}{3}$, E^* *is asymptotically stable for all* $\tau \geq 0$;
- (ii) *When* $\frac{1}{3} < \gamma < 1$, *for case* (i), E^* *is asymptotically stable for* $\tau < \tau_*$ *and unstable for* $\tau > \tau_*$, *and system* (3.1) *undergoes Hopf bifurcation at* $\tau = \tau_{k,j}$;
- (iii) *For case* (ii), *system* (3.1) *undergoes Turing-Hopf bifurcation at* $\tau = \tau_{k,j}$, *with* $0 \leq k \leq k_c^*, k, j \in \mathbb{N}_0$ *and* $k \neq k_*$.

About the complete ordering of the bifurcation values $\tau_{k,j}$, we have the following result.

Theorem 3.4. *For case* (*i*), *if* $\frac{1}{3} < \gamma \le \frac{1}{2}$, *then* $\tau_{0,j} \le \tau_{1,j} \le \cdots \le \tau_{k_c^*-1,j} \le \tau_{k_c^*,j}$, $j \in \mathbb{N}_0$ *and* $\tau_* = \tau_{00}$.

Proof. From (3.27), it is obvious that $\tau_{k,j} < \tau_{k,j+1}$ and $\tau_{k,j}$ is increasing with respect to k provided that $a_{11} + a_{22} \le 0$ and ω_k is decreasing with respect to k. It follows from (3.24) that if P_k and Q_k are increasing with respect to k, ω_k is decreasing in k. By (3.21) and (3.22), we also have

$$\frac{\partial P_k}{\partial k} = 4k\left(\left(d_1^2 + d_2^2\right)k^2 - (d_1 a_{11} + d_2 a_{22})\right)$$

and

$$\frac{\partial Q_k}{\partial k} = 4k\left(d_2 k^2 - a_{22}\right)\left(d_1 k^2 - a_{11}\right)\left(2d_1 d_2 k^2 - (d_1 a_{22} + d_2 a_{11})\right).$$

Notice that $a_{22} = -\delta < 0$. Then, if $a_{11} \le 0$, then $a_{11} + a_{22} \le 0$ and $\partial P_k/\partial k > 0, \partial Q_k/\partial k > 0$. In addition, notice that $a_{11} \le 0$ if and only if $0 < \gamma \le \frac{1}{2}$. This, together with Lemma 3.3, completes the proof. □

In the following, we always assume that $0 < d_1 < d_2$ since we are interested in the delay-induced Turing-Hopf bifurcation.

Theorem 3.5. *For case* (*ii*), *if* $k_c^* = k_*$, *then we have* $\tau_{0,j} \le \tau_{1,j} \le \cdots \le \tau_{k_c^*-1,j}$, $j \in \mathbb{N}_0$ *and then* $\tau_* = \tau_{00}$.

Proof. When (γ, δ) locates on L_{k_*}, we have $1/2 < \gamma < 1$, $a_{11} + a_{22} < 0$, $D_{k_*}(0) = 0$, $D_k(0) > 0$ for $k \ne k_*$ and

$$k_*^2 = \frac{d_2 a_{11} + d_1 a_{22}}{2d_1 d_2}. \tag{3.28}$$

Thus, $d_1 a_{11} + d_2 a_{22} < d_1(a_{11} + a_{22}) < 0$ since $d_1 < d_2$ and $a_{22} = -\delta < 0$. This implies that $\partial P_k/\partial k \ge 0$.

When $k < k_*$, by (3.28) we have

$$d_1 k^2 - a_{11} < d_1 k_*^2 - a_{11} = -\frac{1}{2}a_{11} + \frac{d_1}{2d_2}a_{22} < -\frac{1}{2}a_{11} < 0, \tag{3.29}$$

due to $a_{22} < 0$ and $a_{11} > 0$ for $1/2 < \gamma < 1$.

It follows from (3.28) that

$$2d_1 d_2 k^2 - (d_1 a_{22} + d_2 a_{11}) \begin{cases} < 0, \ 0 \le k < k_*, \\ = 0, \ k = k_*, \\ > 0, \ k > k_*. \end{cases} \tag{3.30}$$

By (3.29) and (3.30), we can conclude that $\partial Q_k/\partial k \ge 0$ for $0 \le k \le k_*$. Therefore, if $k_c^* = k_*$, then the conclusion is immediately confirmed. □

Theorem 3.6. *For case* (*ii*), *if* $\tau_* = \tau_{00}$, *then the characteristic equation* (3.4) *has a pair of purely imaginary roots* $\pm i\omega_0$ *for* $k = 0$ *and a simple zero root for* $k = k_*$, *no roots with zero real parts for* $k \ne 0$ *and* $k \ne k_*$. *In addition, all the roots of* (3.4) *except* $\pm i\omega_0$ *and a simple zero have negative real parts.*

Proof. It follows from Theorem 3.2 that the curve L_{k_*} is the boundary of the stability region for the positive equilibrium E^* of (3.9). And from Lemma 3.2, when $\beta = d_2/d_1 > 1$ and (γ, δ) locates on the Turing bifurcation curve L_{k_*}, the characteristic equations (3.4) with $\tau = 0$ has a simple zero root $\lambda = 0$ when $k = k_*$, no root with zero real parts when $k \in \mathbb{N}_0$ and $k \neq k_*$. Noticing τ_* is the minimal critical value and the transversality condition shown in Lemma 3.4, the proof is complete. □

3.3. Dynamical classification near delay-induced Turing-Hopf bifurcation point

In this subsection, we investigate the dynamical classification near the Turing-Hopf bifurcation point using the normal form theory of Turing-Hopf bifurcation of reaction-diffusion equations with delay developed in Section 2. Choosing δ and τ as bifurcation parameter and assuming that system (3.1) undergoes Turing-Hopf bifurcation at $(\tau, \delta) = (\tau_*, \delta_*)$.

3.3.1. Normal form and dynamical classification

Introduce the perturbation parameters μ_1 and μ_2 by setting $\mu_1 = \delta - \delta_*,\ \mu_2 = \tau - \tau_*$ such that $\mu = (\mu_1, \mu_2) = (0, 0)$ is the value of Turing-Hopf bifurcation.

Setting $\tilde{u}(\cdot, t) = u(\cdot, \tau t) - u^*,\ \tilde{v}(\cdot, t) = v(\cdot, \tau t) - v^*,\ U(t) = (\tilde{u}(\cdot, t), \tilde{v}(\cdot, t))$ and then dropping the tildes for simplicity, (3.1) can be rewritten as the following system in the space $\mathscr{C} = C\left([-1, 0], \mathscr{X}\right)$

$$\frac{dU(t)}{dt} = \tau_* d\Delta U(t) + L_0(U_t) + F(U_t, \mu), \tag{3.31}$$

with

$$F(U_t, \mu) = \mu_2 d\Delta\varphi(0) + L(\mu)(\varphi) + f(\varphi, \mu),$$

where for $\varphi = (\varphi_1, \varphi_2)^T \in \mathcal{C},\ L(\mu_2)(.) : \mathcal{C} \to X$, and $f : \mathcal{C} \times R \to X$ are given, respectively, by

$$L_0(\varphi) = \tau_* \begin{pmatrix} a_{11}\varphi_1(0) + a_{12}\varphi_2(-1) \\ a_{21}(\delta_*)\varphi_1(0) + a_{22}(\delta_*)\varphi_2(0) \end{pmatrix},$$

$$f(\varphi, \mu) = (\tau_* + \mu_2) \begin{pmatrix} \sum\limits_{i+j+k+l \geq 2} \frac{1}{i!j!k!l!} f^{(1)}_{ijkl} \varphi_1^i(0)\varphi_2^j(0)\varphi_2^k(-1)\mu_1^l \\ \sum\limits_{i+j+k+l \geq 2} \frac{1}{i!j!k!l!} f^{(2)}_{ijkl} \varphi_1^i(0)\varphi_2^j(0)\varphi_2^k(-1)\mu_1^l \end{pmatrix}, \tag{3.32}$$

where a_{12} and a_{21} are defined by (3.3), $a_{21}(\delta_*) = \gamma\delta_*, a_{22}(\delta_*) = -\delta_*$,

$$f^{(1)}_{ijkl} = \frac{\partial^{i+j+k+l} f^{(1)}}{\partial u^i \partial v^k \partial w^k \partial \mu_1^l}\left(0, 0, 0, 0\right),\ f^{(2)}_{ijkl} = \frac{\partial^{i+j+k+l} f^{(2)}}{\partial u^i \partial v^k \partial w^k \partial \mu_1^l}\left(0, 0, 0, 0\right)$$

where

$$\begin{cases} f^{(1)}(u, v, w, \mu_1) = (u + u^*)^2\left(1 - (u + u^*)\right) - (u + u^*)\left(w + v^*\right), \\ f^{(2)}(u, v, w, \mu_1) = (\delta^* + \mu_1)\left(v + v^*\right)\left(1 - \frac{v+v^*}{\gamma(u+u^*)}\right). \end{cases} \tag{3.33}$$

Notice that $k=0, k_*>0$ in the Turing-Hopf bifurcation. By a straightforward calculation, we obtain

$$\Phi_1(\theta)=\left(\xi_0 e^{i\omega_c\theta}, \overline{\xi_0} e^{-i\omega_c\theta}\right),\ \Phi_2(\theta)=\xi_{k_*},$$
$$\Psi_1(s)=\operatorname{col}\left(\eta_0^T e^{-i\omega_c s}, \overline{\eta_0}^T e^{i\omega_c s}\right),\ \Psi_2(s)=\eta_{k_*}^T,$$

where $\omega_c=\omega_0\tau_*$,

$$\xi_0=\begin{pmatrix}\xi_{01}\\ \xi_{02}\end{pmatrix}=\begin{pmatrix}1\\ \frac{i\omega_0-a_{11}}{a_{12}}e^{i\omega_c}\end{pmatrix},\ \eta_0=\begin{pmatrix}\eta_{01}\\ \eta_{02}\end{pmatrix}=D_1\begin{pmatrix}1\\ \frac{i\omega_0-a_{11}}{a_{21}(\delta_*)}\end{pmatrix},$$

$$\xi_{k_*}=\begin{pmatrix}\xi_{k_*1}\\ \xi_{k_*2}\end{pmatrix}=\begin{pmatrix}1\\ \frac{d_1k_*^2-a_{11}}{a_{12}}\end{pmatrix},\ \eta_{k_*}=\begin{pmatrix}\eta_{k_*1}\\ \eta_{k_*2}\end{pmatrix}=D_2\begin{pmatrix}\frac{d_2k_*^2-a_{22}(\delta_*)}{a_{12}}\\ 1\end{pmatrix},$$

with

$$D_1=\left(1+\tau_*\left(i\omega_0-a_{11}\right)+\frac{\left(i\omega_0-a_{11}\right)^2}{a_{12}a_{21}\left(\delta_*\right)}e^{i\omega_c}\right)^{-1},$$

$$D_2=\left(\frac{\left(d_1+d_2\right)k_*^2-\left(a_{11}+a_{22}\left(\delta_*\right)+\tau_*a_{12}a_{21}\left(\delta_*\right)\right)}{a_{12}}\right)^{-1}.$$

It follows from (3.33) that $f_{ijkl}^{(1)}=0$ for either $i\geq 3$, or $j\geq 1$, or $k\geq 2$, and $f_{ijkl}^{(2)}=0$ for either $j\geq 2$, or $k\geq 1$, and then by (2.21) and (2.24), we have

$$A_{200}=\tau_*\begin{pmatrix}f_{2000}^{(1)}\xi_{01}^2+2f_{1010}^{(1)}\xi_{01}\xi_{02}e^{-i\omega_c}\\ f_{2000}^{(2)}\xi_{01}^2+2f_{1100}^{(2)}\xi_{01}\xi_{02}+f_{0200}^{(2)}\xi_{02}^2\end{pmatrix}=\overline{A_{020}},$$

$$A_{002}=\tau_*\begin{pmatrix}f_{2000}^{(1)}\xi_{k_*1}^2+2f_{1010}^{(1)}\xi_{k_*1}\xi_{k_*2}\\ f_{2000}^{(2)}\xi_{k_*1}^2+2f_{1100}^{(2)}\xi_{k_*1}\xi_{k_*2}+f_{0200}^{(2)}\xi_{k_*2}^2\end{pmatrix},$$

$$A_{110}=\tau_*\begin{pmatrix}2f_{2000}^{(1)}\left|\xi_{01}\right|^2+2f_{1010}^{(1)}\left(\xi_{01}\overline{\xi_{02}}e^{i\omega_c}+\overline{\xi_{01}}\xi_{02}e^{-i\omega_c}\right)\\ 2f_{2000}^{(2)}\left|\xi_{01}\right|^2+2f_{1100}^{(2)}\left(\xi_{01}\overline{\xi_{02}}+\overline{\xi_{01}}\xi_{02}\right)+2f_{0200}^{(2)}\left|\xi_{02}\right|^2\end{pmatrix},$$

$$A_{101}=\tau_*\begin{pmatrix}2f_{2000}^{(1)}\xi_{01}\xi_{k_*1}+2f_{1010}^{(1)}\left(\xi_{01}\xi_{k_*2}+\xi_{k_*1}\xi_{02}e^{-i\omega_c}\right)\\ 2f_{2000}^{(2)}\xi_{01}\xi_{k_*1}+2f_{1100}^{(2)}\left(\xi_{01}\xi_{k_*2}+\xi_{k_*1}\xi_{02}\right)+2f_{0200}^{(2)}\xi_{02}\xi_{k_*2}\end{pmatrix},$$

and

$$A_{210}=\tau_*\begin{pmatrix} 3f_{3000}^{(1)}\xi_{01}^2\overline{\xi_{01}} \\ 3f_{3000}^{(2)}\xi_{01}^2\overline{\xi_{01}}+f_{2100}^{(2)}\left(\xi_{01}^2\overline{\xi_{02}}+2\left|\xi_{01}\right|^2\xi_{02}\right)+f_{1200}^{(2)}\left(\xi_{01}\xi_{02}^2+2\xi_{01}\left|\xi_{02}\right|^2\right)\end{pmatrix},$$

$$A_{102}=\tau_*\begin{pmatrix} 3f_{3000}^{(1)}\xi_{01}\xi_{k_*1}^2 \\ 3f_{3000}^{(2)}\xi_{01}\xi_{k_*1}^2+f_{2100}^{(2)}\left(\xi_{02}\xi_{k_*1}^2+2\xi_{01}\xi_{k_*1}\xi_{k_*2}\right)+f_{1200}^{(2)}\left(\xi_{01}\xi_{k_*2}^2+2\xi_{02}\xi_{k_*1}\xi_{k_*2}\right)\end{pmatrix},$$

$$A_{111}=\tau_*\begin{pmatrix} 6f_{3000}^{(1)}|\xi_{01}|^2\xi_{k_*1} \\ 6f_{3000}^{(2)}|\xi_{01}|^2\xi_{k_*1}+2f_{2100}^{(2)}\left(|\xi_{01}|^2\xi_{k_*2}+\xi_{01}\overline{\xi_{02}}\xi_{k_*1}+\overline{\xi_{01}}\xi_{02}\xi_{k_*1}\right) \\ +2f_{1200}^{(2)}\left(|\xi_{02}|^2\xi_{k_*1}+\xi_{01}\overline{\xi_{02}}\xi_{k_*2}+\overline{\xi_{01}}\xi_{02}\xi_{k_*2}\right)\end{pmatrix},$$

$$A_{003}=\tau_*\begin{pmatrix} f_{3000}^{(1)}\xi_{k_*1}^3 \\ f_{3000}^{(2)}\xi_{k_*1}^3+f_{2100}^{(2)}\xi_{k_*1}^2\xi_{k_*2}+f_{1200}^{(2)}\xi_{k_*1}\xi_{k_*2}^2\end{pmatrix}.$$

Thus, $h_{ijkl}(\theta)$ can be obtain by (2.33) (2.34) and (2.35). Then, by (2.21) and (3.33), we have

$$\mathcal{S}_2\left(\xi_0e^{i\omega_c\theta},h_{0110}\right)=2\tau_*\begin{pmatrix} f_{2000}^{(1)}\xi_{01}h_{0110}^{(1)}(0)+vf_{1010}^{(1)}\left(p_{01}h_{0110}^{(2)}(-1)+\xi_{02}e^{-i\omega\tau_*}h_{0110}^{(1)}(0)\right) \\ f_{2000}^{(2)}\xi_{01}h_{0110}^{(1)}(0)+f_{1100}^{(2)}\left(\xi_{01}h_{0110}^{(2)}(0)+\xi_{02}h_{0110}^{(1)}(0)\right)+f_{0200}^{(2)}\xi_{02}h_{0110}^{(2)}(0)\end{pmatrix},$$

$$\mathcal{S}_2\left(\overline{\xi_0}e^{-i\omega_c\theta},h_{0200}\right)=2\tau_*\begin{pmatrix} f_{2000}^{(1)}\overline{\xi_{01}}h_{0200}^{(1)}(0)+f_{1010}^{(1)}\left(\overline{\xi_{01}}h_{0200}^{(2)}(-1)+\overline{\xi_{02}}e^{i\omega\tau_*}h_{0200}^{(1)}(0)\right) \\ f_{2000}^{(2)}\overline{\xi_{01}}h_{0200}^{(1)}(0)+f_{1100}^{(2)}\left(\overline{\xi_{01}}h_{0200}^{(2)}(0)+\overline{\xi_{02}}h_{0200}^{(1)}(0)\right)+f_{0200}^{(2)}\overline{\xi_{02}}h_{0200}^{(2)}(0)\end{pmatrix},$$

$$\mathcal{S}_2\left(\xi_0e^{i\omega_c\theta},h_{0002}\right)=2\tau_*\begin{pmatrix} f_{2000}^{(1)}\xi_{01}h_{0002}^{(1)}(0)+f_{1010}^{(1)}\left(\xi_{01}h_{0002}^{(2)}(-1)+\xi_{02}e^{-i\omega\tau_*}h_{0002}^{(1)}(0)\right) \\ f_{2000}^{(2)}\xi_{01}h_{0002}^{(1)}(0)+f_{1100}^{(2)}\left(\xi_{01}h_{0002}^{(2)}(0)+\xi_{02}h_{0002}^{(1)}(0)\right)+f_{0200}^{(1)}\xi_{02}h_{0002}^{(2)}(0)\end{pmatrix},$$

$$\mathcal{S}_2\left(\xi_{k_*},h_{k_*101}\right)=2\tau_*\begin{pmatrix} f_{2000}^{(1)}\xi_{k_*1}h_{k_*101}^{(1)}(0)+f_{1010}^{(1)}\left(\xi_{k_*1}h_{k_*101}^{(2)}(-1)+\xi_{k_*2}h_{k_*101}^{(1)}(0)\right) \\ f_{2000}^{(1)}\xi_{k_*1}h_{k_*101}^{(1)}(0)+f_{1100}^{(2)}\left(\xi_{k_*1}h_{k_*101}^{(2)}(0)+\xi_{k_*2}h_{k_*101}^{(1)}(0)\right) \\ +f_{0200}^{(2)}\xi_{k_*2}h_{k_*101}^{(2)}(0)\end{pmatrix},$$

$$\mathcal{S}_2\left(\xi_0e^{i\omega_c\theta},h_{k^*011}\right)=2\tau_*\begin{pmatrix} f_{2000}^{(1)}\xi_{01}h_{k_*011}^{(1)}(0)+f_{1010}^{(1)}\left(\xi_{01}h_{k_*011}^{(2)}(-1)+\xi_{02}e^{-i\omega\tau_*}h_{k_*011}^{(1)}(0)\right) \\ f_{2000}^{(2)}\xi_{01}h_{k_*011}^{(1)}(0)+f_{1100}^{(2)}\left(\xi_{01}h_{k_*011}^{(2)}(0)+\xi_{02}h_{k_*011}^{(1)}(0)\right) \\ +f_{0200}^{(2)}\xi_{02}h_{k_*011}^{(2)}(0)\end{pmatrix},$$

$$\mathcal{S}_2\left(\overline{\xi_0}e^{-i\omega_c\theta},h_{k_*101}\right)=2\tau_*\begin{pmatrix} f_{2000}^{(1)}\overline{\xi_{01}}h_{k_*101}^{(1)}(0)+f_{1010}^{(1)}\left(\overline{\xi_{01}}h_{k^*101}^{(2)}(-1)+\overline{\xi_{02}}e^{i\omega\tau^*}h_{k^*101}^{(1)}(0)\right) \\ f_{2000}^{(2)}\overline{\xi_{01}}h_{k_*101}^{(1)}(0)+f_{1100}^{(2)}\left(\overline{\xi_{01}}h_{k^*101}^{(2)}(0)+\overline{\xi_{02}}h_{k^*101}^{(1)}(0)\right) \\ +f_{0200}^{(2)}\overline{\xi_{02}}h_{k_*101}^{(2)}(0)\end{pmatrix},$$

$$\mathcal{S}_2\left(\xi_{k_*},h_{0110}\right)=2\tau_*\begin{pmatrix} f_{2000}^{(1)}\xi_{k_*1}h_{0110}^{(1)}(0)+f_{1010}^{(1)}\left(\xi_{k_*1}h_{0110}^{(2)}(-1)+\xi_{k_*2}h_{0110}^{(1)}(0)\right) \\ f_{2000}^{(2)}\xi_{k_*1}h_{0110}^{(1)}(0)+f_{1100}^{(2)}\left(\xi_{k_*1}h_{0110}^{(2)}(0)+\xi_{k_*2}h_{0110}^{(1)}(0)\right) \\ +f_{0200}^{(2)}\xi_{k_*2}h_{0110}^{(2)}(0)\end{pmatrix},$$

$$\mathcal{S}_2\left(\xi_{k_*}, h_{(2k_*)110}\right) = 2\tau_* \begin{pmatrix} f^{(1)}_{2000}\xi_{k_*1}h^{(1)}_{(2k_*)110}(0) + f^{(1)}_{1010}\left(\xi_{k_*1}h^{(2)}_{(2k_*)110}(-1) + \xi_{k_*2}h^{(1)}_{(2k_*)110}(0)\right) \\ f^{(2)}_{2000}\xi_{k_*1}h^{(1)}_{(2k_*)110}(0) + f^{(2)}_{1100}\left(\xi_{k_*1}h^{(2)}_{(2k_*)110}(0) + \xi_{k_*2}h^{(1)}_{(2k_*)110}(0)\right) \\ +f^{(2)}_{0200}\xi_{k_*2}h^{(2)}_{(2k_*)110}(0) \end{pmatrix},$$

$$\mathcal{S}_2\left(\xi_{k_*}, h_{0002}\right) = 2\tau_* \begin{pmatrix} f^{(1)}_{2000}\xi_{k_*1}h^{(1)}_{0002}(0) + f^{(1)}_{1010}\left(\xi_{k_*1}h^{(2)}_{0002}(-1) + \xi_{k_*2}h^{(1)}_{0002}(0)\right) \\ f^{(2)}_{2000}\xi_{k_*1}h^{(1)}_{0002}(0) + f^{(2)}_{1100}\left(\xi_{k_*1}h^{(2)}_{0002}(0) + \xi_{k_*2}h^{(1)}_{0002}(0)\right) \\ +f^{(2)}_{0200}\xi_{k_*2}h^{(2)}_{0002}(0) \end{pmatrix},$$

$$\mathcal{S}_2\left(\xi_{k_*}, h_{(2k_*)002}\right) = 2\tau_* \begin{pmatrix} f^{(1)}_{2000}\xi_{k_*1}h^{(1)}_{(2k_*)002}(0) + f^{(1)}_{1010}\left(\xi_{k_*1}h^{(2)}_{(2k_*)002}(-1) + p_{k_*2}h^{(1)}_{(2k_*)002}(0)\right) \\ f^{(2)}_{2000}\xi_{k_*1}h^{(1)}_{(2k_*)002}(0) + f^{(2)}_{1100}\left(\xi_{k_*1}h^{(2)}_{(2k_*)002}(0) + \xi_{k_*2}h^{(1)}_{(2k_*)002}(0)\right) \\ +f^{(2)}_{0200}\xi_{k_*2}h^{(2)}_{(2k_*)002}(0) \end{pmatrix}.$$

3.3.2. Numerical simulations

Next we provide numerical simulations to support and extend our analytical results. Taking $d_1 = 0.0125, d_2 = 0.125$ as used in Fig.1(B) and choosing the point $P_2(0.7, 0.25)$, i.e., $\gamma = 0.7, \delta = 0.25$, then the positive equilibrium is $E^*(0.3, 0.21)$ and by (3.27) , we have $\tau_{00} = 2.5278$. Then system (3.1) undergoes Turing-Hopf bifurcation at $(\delta_*, \tau_*) = (0.25, 2.5278)$. Using the procedure in Section 2 and Section 3.2.2 with $k_* = 2$, the normal form truncated to the third order terms is

$$\begin{cases} \dot{\rho} = (-0.5310\mu_1 + 0.0538\mu_2)\,\rho - 0.3126\rho^3 + 1.1516\rho r^2, \\ \dot{r} = -0.6466\mu_1 r - 7.1041\rho^2 r - 4.4652r^3. \end{cases} \tag{3.34}$$

Notice that $\rho > 0$ and r is arbitrary real number. System (3.34) has a zero equilibrium $A_0(0,0)$ for any $\mu_1, \mu_2 \in \mathbb{R}$, three boundary equilibria:

$$A_1\left(\sqrt{\frac{-0.5310\mu_1 + 0.0538\mu_2}{0.3126}},\ 0\right),\quad \mu_2 > 9.8699\mu_1,$$

$$A_2^{\pm}\left(0,\ \pm\sqrt{-\frac{0.6466\mu_1}{4.4652}}\right),\ \mu_1 < 0,$$

and two interior equilibria:

$$A_3^{\pm}\left(\sqrt{\frac{-3.1155\mu_1 + 0.2403\mu_2}{9.5767}},\ \pm\sqrt{\frac{3.5698\mu_1 - 0.3824\mu_2}{9.5767}}\right),\ 12.9650\mu_1 < \mu_2 < 9.3353\mu_1, \mu_1 < 0.$$

Define the critical bifurcation lines as follows:

$$\begin{aligned} T:&\ \mu_1 = 0; \\ H_0:&\ \mu_2 = 9.8699\mu_1; \\ T_1:&\ \mu_2 = 9.3353\mu_1,\ \mu_1 < 0; \\ T_2:&\ \mu_2 = 12.9652\mu_1,\ \mu_1 < 0. \end{aligned}$$

These four lines divide the $\mu_1 - \mu_2$ parameter plane into six regions marked as

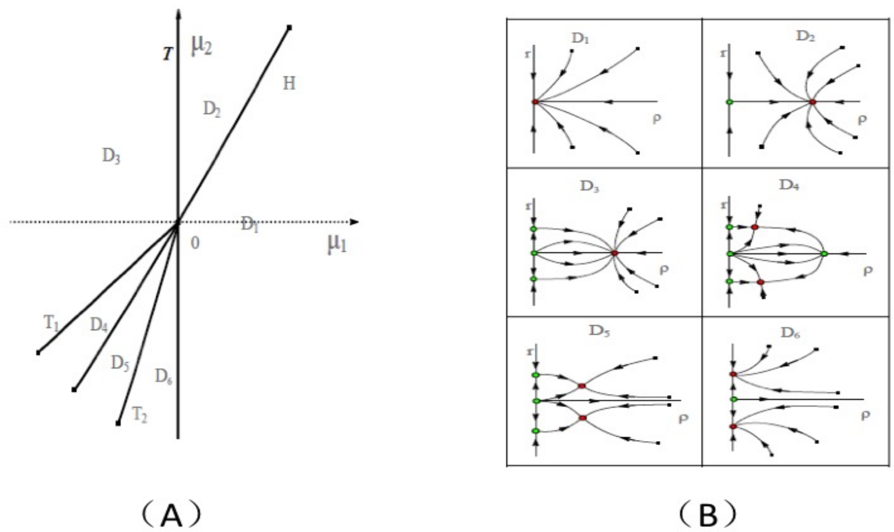

Figure 2. Bifurcation diagrams (A) and dynamical classification (B) near the Turing-Hopf point. μ_1 and μ_2 are the perturbation for the parameters δ and τ, respectively, at $(\delta_*, \tau_*) = (0.25, 2.5278)$.

$D_j, j = 1, 2, \cdots, 6$, in Fig.2(A). By analyzing the stability of these equilibria, the phase portrait of system (3.34) in each region D_j can be shown in Fig.2(B).

The dynmais of the original reaction-diffusion system (3.1) can be determined by the the normal form system (3.34) near the neighbourhood of the Turing-Hopf bifurcation point. We list the corresponding relationship between the equilibrium of (3.34) and the solution of (3.1) in Table 1.

In what follows, we illustrate how the dynamics of system (3.1) changes with the variation of the parameters $\mu_i (i = 1, 2)$. We use the following initial conditions for delayed PDEs

$$u(x, t) = \phi_1(x), v(x, t) = \phi_2(x), \quad t \in [-\tau, 0].$$

and for simplicity of notations, we only write $u(x, 0) = \phi_1(x), v(x, 0) = \phi_2(x)$ for

Table 1. Relationship between the equilibrium of (3.34) and the solution of (3.1)

Equilibrium of (3.34)	Solution of (3.1)
A_0	Constant equilibrium E^*
A_1	Spatially homogeneous periodic solution
$A_2^{\pm}$	Two spatially inhomogeneous steady states with $\cos(2x)$ − like shape
$A_3^{\pm}$	Two spatially inhomogeneous periodic solutions with $\cos(2x)$ − like shape in space

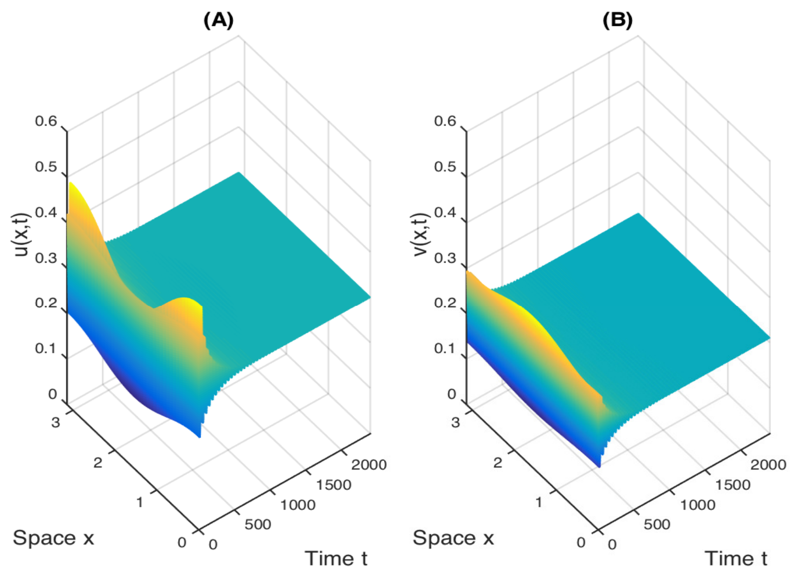

Figure 3. When $(\mu_1, \mu_2) = (0.01, -0.12) \in D_1$, the positive constant equilibrium E^* is asymptotically stable.

these initial conditions.

In region D_1, (3.34) has only one stable zero equilibrium A_0 . Thus, the positive constant equilibrium E^* of system (3.1) is asymptotically stable, as shown in Fig.3 for $(\mu_1, \mu_2) = (0.01, -0.12) \in D_1$ and the initial value $u(x, 0) = 0.3 + 0.02\cos(2x), v(x, 0) = 0.21 - 0.02\cos(2x)$.

When $\mu_i (i = 1, 2)$ varies from the region D_1 to D_2, A_0 loses its stability and one stable boundary equilibrium A_1 emerges in the μ_1-axis. This means that the positive equilibrium E^* of system (3.1) becomes unstable and the stable spatially homogeneous periodic solution emerges, as shown in Fig.4 for $(\mu_1, \mu_2) = (0.01, 0.5) \in D_2$ and the same initial value as in Fig.3.

Altering μ_i from the region D_2 to D_3, A_1 remains stable and two unstable equilibria $A_2^{\pm}$ are born in the μ_2-axis, which are saddle, implying there exist the heteroclinic orbits connecting equilibria $A_2^{\pm}$ to stable boundary equilibrium A_1. So, the stable spatially homogeneous periodic solution of system (3.1) remains in this region and there exists the connecting orbit from the unstable inhomogeneous steady state to stable spatially homogeneous periodic solution. The unstable equilibria $A_2^{\pm}$ means that system (3.1) has two unstable spatially inhomogeneous steady states with $\cos(2x)$ − like shape. Taking $(\mu_1, \mu_2) = (-0.01, 0.01) \in D_3$ and the initial value $u(x, 0) = 0.3 - 0.006\cos(2x), v(x, 0) = 0.21 - 0.02\cos(2x)$ closing to one of these two inhomogeneous steady states, Fig.5 shows the evolution of the solution of system (3.1) . (A,D) depicts the short-term behaviour, (B,E) shows the middle-term behaviour and (C,F) is the long-term behaviour. Same notation is used in Figs.6-9.

When the parameters vary from the region D_3 to D_4, A_1 of (3.34) loses its stability and two stable interior eqilibria $A_3^{\pm}$ emerge. Taking $(\mu_1, \mu_2) = (-0.01, -0.095) \in D_4$ and the initial condtion $u(x, 0) = 0.3-0.01\cos(2x), v(x, 0) = 0.21+0.002\cos(2x)$

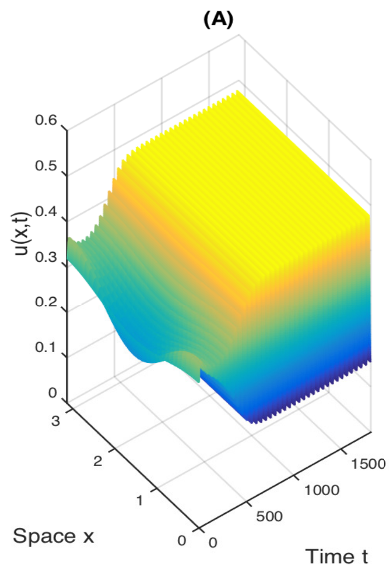

Figure 4. When $(\mu_1, \mu_2) = (0.01, 0.5) \in D_2$, the positive constant equilibrium E^* is unstable and there is a stable spatially homogeneous periodic solution.

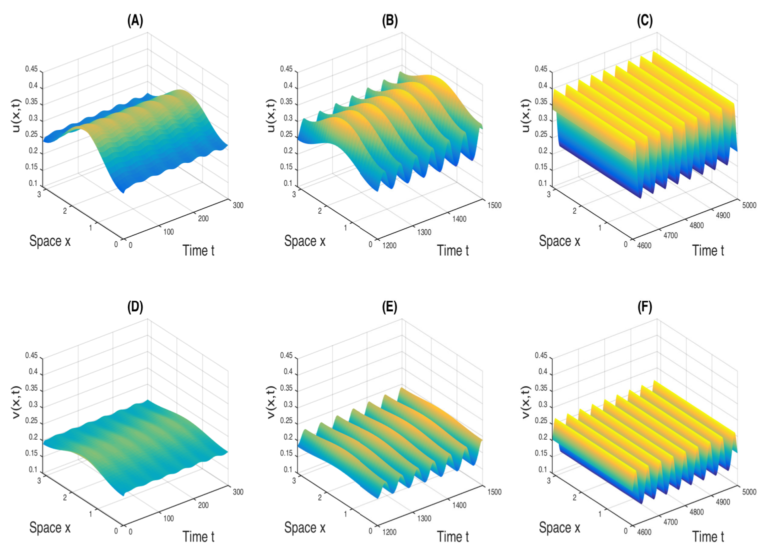

Figure 5. When $(\mu_1, \mu_2) = (-0.01, 0.01) \in D_3$, there are unstable spatially inhomogeneous steady states, stable spatially homogeneous periodic solution and there exists a orbit connecting these two states.

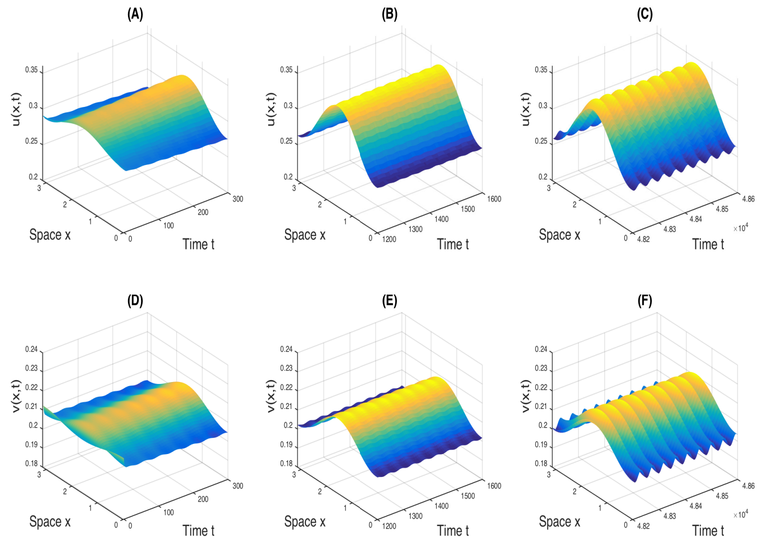

Figure 6. When $(\mu_1, \mu_2) = (-0.01, -0.095) \in D_4$, there are unstable spatially inhomogeneous steady states and stable spatially inhomogeneous periodic solutions. For the initial condtion $u(x, 0) = 0.3 - 0.01\cos(2x), v(x, 0)) = 0.21 + 0.002\cos(2x)$, there is a transition from unstable spatially inhomogeneous steady state to stable spatially inhomogeneous periodic solution.

close to the unstable inhomogeneous steady state, Fig.6 numerically shows the existence of the stable spatially inhomogeneous periodic solution and the transition from the unstable inhomogeneous steady state to stable spatially inhomogeneous periodic solution.

With the same values of μ_i as in Fig.6 and choosing different initial condtion as $u(x, 0) = 0.3 - 0.01, v(x, 0) = 0.21 + 0.001\cos(2x)$, the short-term behaviour (Figs.7 (A,D) seems like spatially homogeneous periodic solution, which are differet from that shown in Figs.6 (A,D). Then, with the increasing of time, the spatial heterogeneity appears (Figs.7 (B,E)) and the system finally evolves into stable spatially inhomogeneous periodic solution (Figs.7 (C,F)). As shown in Fig.2(B) and Table 1, when $(\mu_1, \mu_2) \in D_4$, system (3.1) has two stable spatially inhomogeneous periodic solutions. Choosing another initial condtion $u(x, 0) = 0.3 - 0.01, v(x, 0) = 0.21 - 0.001\cos(2x)$, Fig.8 shows that system (3.1) finally evolves into another stable spatially inhomogeneous periodic solution (Figs.8(C,F)).

Moving from the region D_4 to D_5, A_1 disappears and $A_3^{\pm}$ remain stable. For system (3.1), Fig.9 shows the existence of stable spatially inhomogeneous periodic solution and the transition from the unstable inhomogeneous steady state to stable spatially inhomogeneous periodic solution for $(\mu_1, \mu_2) = (-0.01, -0.1) \in D_5$ and the initial value $u(x, 0) = 0.3 - 0.02\cos(2x), v(x, 0) = 0.21 - 0.01\cos(2x)$.

In region D_6, the normal form system (3.34) has one unstable zero equilibrium A_0 and two stable boundary equilibria $A_2^{\pm}$ in the μ_2-axis. This implies that the positive equilibrium E^* of system (3.1) is unstable and there have two stable inhomogeneous steady states. Choosing $(\mu_1, \mu_2) = (-0.01, -0.5) \in D_6$ and the initial condtion $u(x, 0) = 0.3 - 0.04\cos(2x), v(x, 0) = 0.21 + 0.01\cos(2x)$, Fig.10 shows the existence of the stable spatially inhomogeneous steady state.

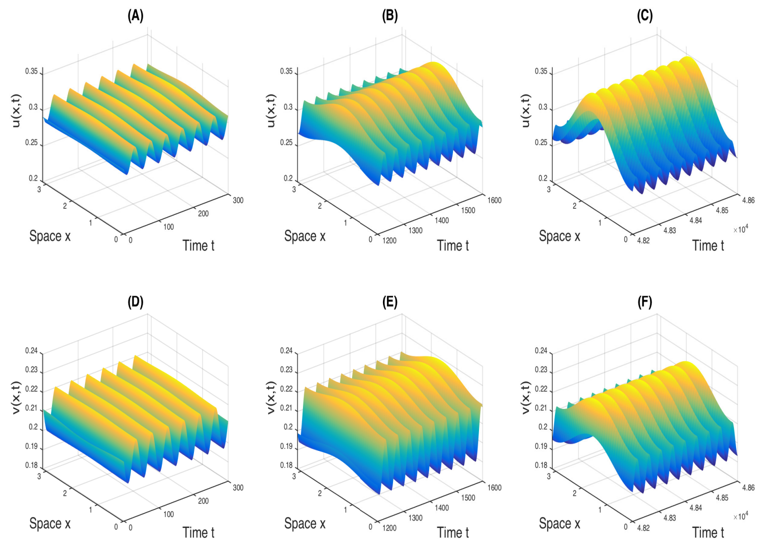

Figure 7. When $(\mu_1, \mu_2) = (-0.01, -0.095) \in D_4$, there are unstable spatially inhomogeneous steady states and stable spatially inhomogeneous periodic solutions. For the initial condtion $u(x, 0) = 0.3 - 0.01, v(x, 0)) = 0.21 + 0.001 \cos(2x)$, there is a transition from unstable spatially homogeneous periodic solution to stable spatially inhomogeneous periodic solution.

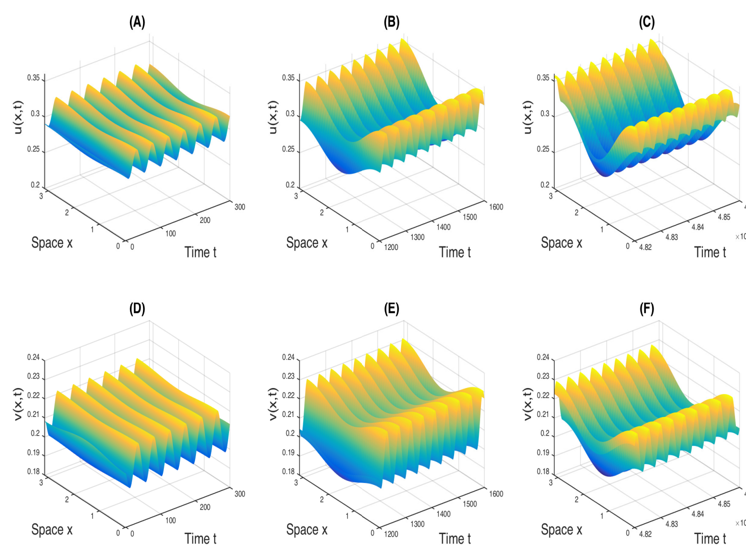

Figure 8. When $(\mu_1, \mu_2) = (-0.01, -0.095) \in D_4$, there are unstable spatially inhomogeneous steady states and stable spatially inhomogeneous periodic solutions. For the initial condtion $u(x, 0) = 0.3 - 0.01, v(x, 0)) = 0.21 - 0.001 \cos(2x)$, there is another stable spatially inhomogeneous periodic solution, which is different from that shown in Fig.7 .

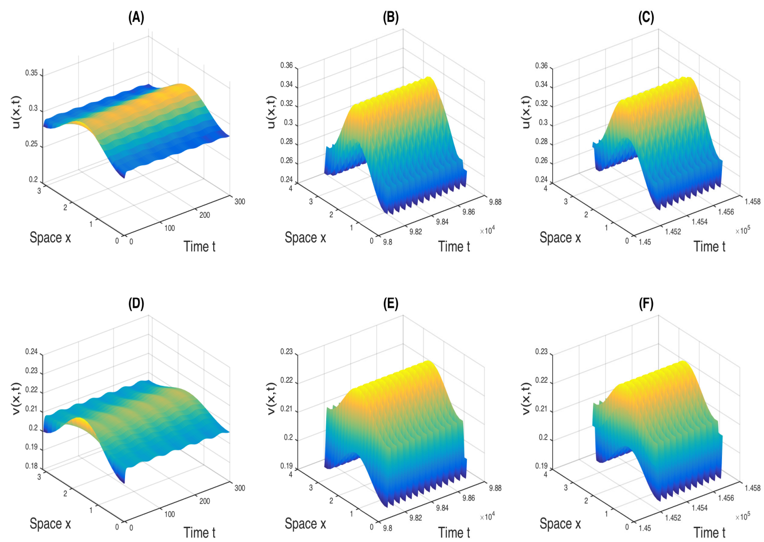

Figure 9. When $(\mu_1, \mu_2) = (-0.01, -0.1) \in D_5$, there are unstable spatially inhomogeneous steady states and stable spatially inhomogeneous periodic solutions.

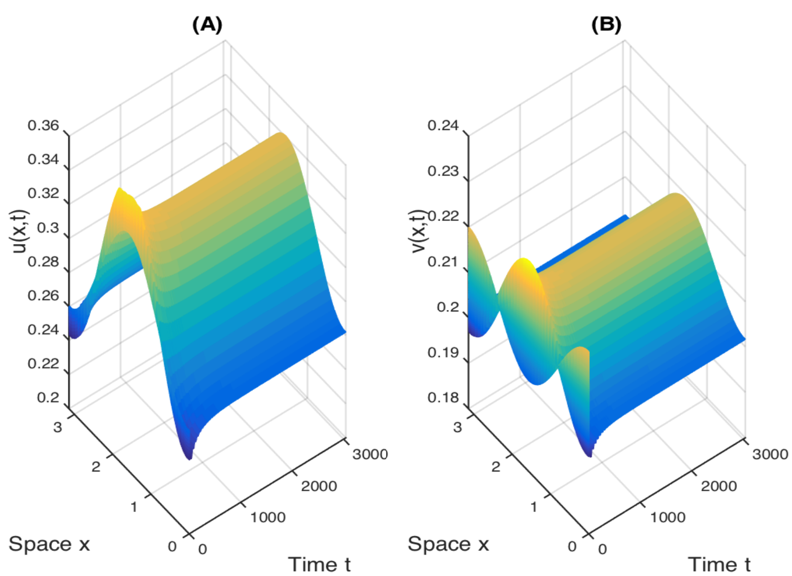

Figure 10. When $(\mu_1, \mu_2) = (-0.01, -0.5) \in D_6$, the positive constant equilibrium is unstable and there is stable spatially inhomogeneous steady states with $\cos(2x) -$ like shape.

4. Conclusion

In this paper, we consider the Turing-Hopf bifurcation in the reaction-diffusion system with delay. The algorithm of normal form corresponding to Turing-Hopf bifurcation is analytically derived. As an application, we investigate the dynamics of the diffusive predator-prey model with weak Allee effect and delay. The stability, diffusion-driven instability, Hopf bifurcation and Turing-Hopf bifurcation are studied. Especially, the dynamical classification near Turing-Hopf bifurcation point can be explicitly determined by applying our algorithm. The stable spatially homogeneous/inhomogeneous steady states and periodic solutions are found. We show that there exist different heteroclinic orbits from spatially homogeneous/inhomogeneous steady state to spatially homogeneous/inhomogeneous periodic solution, and from spatially homogeneous periodic solution to spatially inhomogeneous periodic solution. To the best of our knowledge, the heteroclinic orbits in the reaction-diffusion system with delay has not been reported in the literatures. The theoretical results develped in this paper is helpful to understand deeply the complex dynamics due to the interaction of diffusion-driven Turing instability and delay-induced Hopf bifurcation. We would like to mention that the results related to Turing-Hopf bifurcation in this paper is dealt under the Neumann boundary condition but also applicable for the case of Direchlet boundary condition. For the application, although we present the results mainly for the diffusive predator-prey model with weak Allee effect and delay, we believe some other application models can be studied in a similar manner.

The influence of the nonlocal intraspecific competition of the prey on the spatiotemporal dynamics of the diffusive predator-prey model has been recently investigated in [5, 44]. The extension of this paper to the case with delay and nonlocal term is interesting and in progress.

Acknowledgements. The authors are grateful to the anonymous referees for their useful suggestions which improve the contents of this article.

References

[1] S. Busenberg and W. Huang, *Stability and Hopf bifurcation for a population delay model with diffusion effects*, J. Diff. Eqs., 1996, 124(1), 80–107.

[2] J. Cao, P. Wang, R. Yuan and Y. Mei, *Bogdanov–Takens Bifurcation of a Class of Delayed Reaction–Diffusion System*, Internat. J. Bifur. Chaos, 2015, 25(06), 1550082.

[3] S. Chen and J. Shi, *Stability and Hopf bifurcation in a diffusive logistic population model with nonlocal delay effect*, J. Diff. Eqs., 2012, 253(12), 3440–3470.

[4] S. Chen, J. Shi and J. Wei, *Global stability and Hopf bifurcation in a delayed diffusive Leslie-Gower predator-prey system*, Internat. J. Bifur. Chaos, 2012, 22(03), 1250061.

[5] S. Chen and J. Yu, *Stability and bifurcation on predator-prey systems with nonlocal prey competition*, Discrete Contin. Dyn. Syst., 2018, 38(1), 43–62.

[6] Y. Dong, S. Li and S. Zhang, *Hopf bifurcation in a reaction-diffusion model with degn–harrison reaction scheme*, Nonlinear Anal. Real World Appl., 2017, 33, 284–297.

[7] L. Du and M. Wang, *Hopf bifurcation analysis in the 1-D Lengyel–Epstein reaction–diffusion model*, J. Math. Anal. Appl., 2017, 366(2), 473–485.

[8] T. Faria, *Normal forms and Hopf bifurcation for partial differential equations with delays*, Trans. Amer. Math. Soc., 2000, 352(5), 2217–2238.

[9] T. Faria, *Stability and bifurcation for a delayed predator–prey model and the effect of diffusion*, J. Math. Anal. Appl., 2001, 254(2), 433–463.

[10] E. González-Olivares and A. Rojas-Palma, *Multiple limit cycles in a Gause type predator–prey model with Holling type III functional response and Allee effect on prey*, B. Math. Biol., 2011, 73(6), 1378–1397.

[11] S. Guo, *Stability and bifurcation in a reaction-diffusion model with nonlocal delay effect*, J. Diff. Eqs., 2015, 259(4), 1409–1448.

[12] S. Guo and L. Ma, *Stability and bifurcation in a delayed reaction-diffusion equation with Dirichlet boundary condition*, J. Nonlinear Sci., 2016, 26(2), 545–580.

[13] K. P. Hadeler and S. Ruan, *Interaction of diffusion and delay*, Discrete Contin. Dyn. Syst. Ser. B, 2007, 8(1), 95–105.

[14] M. Haragus and G. Iooss, *Local bifurcations, center manifolds, and normal forms in infinite-dimensional dynamical systems*, Springer, London, 2010.

[15] R. Hu and Y. Yuan, *Spatially nonhomogeneous equilibrium in a reaction-diffusion system with distributed delay*, J. Diff. Eqs., 2011, 250(6), 2779–2806.

[16] R. Hu and Y. Yuan, *Stability and Hopf bifurcation analysis for Nicholson's blowflies equation with non-local delay*, European J. Appl. Math., 2012, 23(6), 777–796.

[17] W. Jiang, Q. An and J. Shi, *Formulation of the normal forms of Turing-Hopf bifurcation in reaction-diffusion systems with time delay.* https://arxiv.org/abs/1802.10286

[18] J. Jin, J. Shi, J. Wei and F.Yi, *Bifurcations of patterned solutions in the diffusive Lengyel-Epstein system of CIMA chemical reactions*, Rocky Mountain J. Math., 2013, 43(5), 1637–1674.

[19] W. Just, M. Bose, S. Bose, H. Engel and E.Schöll, *Spatiotemporal dynamics near a supercritical Turing-Hopf bifurcation in a two-dimensional reaction-diffusion system*, Physical Rev. E, 2001, 64, 026219.

[20] H. Kidachi, *On mode interactions in reaction-diffusion equation with nearly degenerate bifurcations*, Prog. Theoret. Phy., 1980, 63, 1152–1169.

[21] S. Kondo and T. Miura, *Reaction-Diffusion Model as a Framework for Understanding Biological Pattern Formation*, Science, 2010, 329(5999), 1616–1620.

[22] Y. Lv, Y. Pei and R. Yuan, *Hopf bifurcation and global stability of a diffusive Gause-type predator–prey models*, Comput. Math. Appl., 2016, 72(10), 2620–2635.

[23] Z. Mei, *Numerical Bifurcation Analysis for Reaction-Diffusion Equations*, Springer-Verlag, Berlin, 2000.

[24] M. C. Memory, *Bifurcation and asymptotic behavior of solutions of a delay-differential equation with diffusion*, SIAM J. Math. Anal., 1989, 20(3), 533–546.

[25] P. J. Pal, T. Saha, M. Sen and M. Banerjee, *A delayed predator–prey model with strong allee effect in prey population growth*, Nonlinear Dynam., 2012, 68(1), 23–42.

[26] J. E. Pearson, *Complex patterns in a simple system*, Science, 1993, 261(5118), 189–192.

[27] Y. Peng and H. Ling, *Pattern formation in a ratio-dependent predator-prey model with cross-diffusion*, Appl. Math. Comput., 2018, 331, 307–318.

[28] Y. Peng and T. Zhang, *Turing instability and pattern induced by cross-diffusion in a predator-prey system with Allee effect*, Appl. Math. Comput., 2016, 275, 1–12.

[29] H. Shi and S. Ruan, *Spatial, temporal and spatiotemporal patterns of diffusive predator–prey models with mutual interference*, IMA J. Appl. Math., 2015, 80(5), 1534–1568.

[30] Q. Shi, J. Shi and Y. Song, *Hopf bifurcation in a reaction-diffusion equation with distributed delay and Dirichlet boundary condition*, J. Diff. Eqs., 2017, 263(10), 6537–6575.

[31] J. Shi, Z. Xie and K. Little, *Cross-diffusion induced instability and stability in reaction-diffusion systems*, J. Appl. Anal. Comput., 2011, 1(1), 95–119.

[32] Y. Song, H. Jiang, Q. Liu and Y. Yuan, *Spatiotemporal Dynamics of the Diffusive Mussel-Algae Model Near Turing-Hopf Bifurcation*, SIAM J. Appl. Dyn. Syst., 2017, 16(4), 2030–2062.

[33] Y. Song and J. Jiang, *Hopf and steady-state-Hopf bifurcations in delay differential equations with applications to a damped harmonic oscillator with delay feedback*, Internat. J. Bifur. Chaos, 2012, 22(12), 1250286.

[34] Y. Song, T. Zhang and Y. Peng, *Turing-Hopf bifurcation in the reaction-diffusion equations and its applications*, Commun. Nonlinear Sci. Numer. Simul., 2016, 33, 229–258.

[35] Y. Su, J. Wei and J. Shi, *Hopf bifurcations in a reaction-diffusion population model with delay effect*, J. Diff. Eqs., 2009, 247(4), 1156–1184.

[36] Y. Su and X. Zou, *Transient oscillatory patterns in the diffusive non-local blowfly equation with delay under the zero-flux boundary condition*, Nonlinearity, 2014, 27(1), 87–104.

[37] X. Tang and Y. Song, *Stability, Hopf bifurcations and spatial patterns in a delayed diffusive predator-prey model with herd behavior*, Appl. Math. Comput., 2015, 254, 375–391.

[38] A. M. Turing, *The chemical basis of morphogenesis*, Philos. Trans. Roy. Soc. London Ser. B, 1952, 237(641), 37–72.

[39] V. K. Vanag and I. R. Epstein, *Pattern formation mechanisms in reaction-diffusion systems*, Int. J. Dev. Biol., 2009, 53(5–6), 673–681.

[40] A. I. Volpert, Vitaly Volpert and V. A. Volpert, *Traveling wave solutions of parabolic systems*, vol. 140, American Mathematical Soc., 1994.

[41] W. Wang, X. Gao, Y. Cai, H. Shi and S. Fu, *Turing patterns in a diffusive epidemic model with saturated infection force*, J. Franklin. Inst., 2018, 355, 7226–7245.

[42] J. Wang, J. Liang, Y. Liu and J. Wang, *Zero singularities of codimension two in a delayed predator-prey diffusion system*, Neurocomputing, 2017, 227, 10–17.

[43] J. Wang, J. Shi and J. Wei, *Predator-prey system with strong allee effect in prey*, J. Math. Biol., 2011, 62(3), 291–331.

[44] S. Wu and Y. Song, *Stability and spatiotemporal dynamics in a diffusive predator-prey model with nonlocal prey competition*, Nonlinear Anal. Real World Appl., 2019, 48, 12–39.

[45] H. Wu and X. Wu, *Bogdanov–Takens singularity for a system of reaction-diffusion equations*, J. Math. Chem., 2016, 54(1), 120–136.

[46] J. Wu and X. Zou, *Traveling wave fronts of reaction-diffusion systems with Delay*, J. Dynam. Differential Equations, 2001, 13(3), 651–687.

[47] R. Yang and Y. Song, *Spatial resonance and Turing-Hopf bifurcations in the Gierer-Meinhardt model*, Nonlinear Anal. Real World Appl., 2016, 31, 356–387.

[48] T. Zhang, X. Liu, X. Meng and T. Zhang, *Spatio-temporal dynamics near the steady state of a planktonic system*, Comput. Math. Appl., 2018, 75(12), 4490–4504.

[49] F. Yi, J. Wei and J. Shi, *Bifurcation and spatiotemporal patterns in a homogeneous diffusive predator–prey system*, J. Diff. Eqs., 2009, 246(5), 1944–1977.

[50] W. Zuo and J. Wei, *Stability and Hopf bifurcation in a diffusive predator-prey system with delay effect*, Nonlinear Anal. Real World Appl., 2011, 12(4), 1998–2011.